**Secreted long non-coding RNAs *Gadlor1* and *Gadlor2* affect multiple cardiac cell types and aggravate cardiac remodeling during pressure overload**

Merve Keles, MSc[1,2,3]*, Steve Grein, MSc[1,3]*, Natali Froese, PhD[4], Dagmar Wirth, PhD[5], Felix A. Trogisch, PhD[1,2,3], Rhys Wardman, PhD[1,3], Shruthi Hemanna, MSc[1,3], Nina Weinzierl, BSc[1], Stefanie Uhlig, BSc[6], Santosh Lomada, PhD[3,7], Gesine M. Dittrich, MD[1,3], Malgorzata Szaroszyk, PhD[4], Ricarda Haustein, MD[4], Jan Hegermann, PhD[8], Abel Martin-Garrido, PhD[1], Johann Bauersachs, MD[4], Derk Frank, MD[9], Norbert Frey, MD[10], Karen Bieback, PhD[6], Julio Cordero, PhD[11], Gergana Dobreva, PhD[3,11], Thomas Wieland, PhD[3,7] and Joerg Heineke, MD[1,2,3]

[1]ECAS (European Center for Angioscience), Department of Cardiovascular Physiology, Medical Faculty Mannheim of Heidelberg University, Mannheim, Germany;

[2]CFPM (Core Facility Platform Mannheim), Cardiac Imaging Center, Medical Faculty Mannheim of Heidelberg University, Mannheim, Germany;

[3]DZHK (German Center for Cardiovascular Research), partner site Heidelberg/Mannheim, Mannheim, Germany;

[4]Department of Cardiology and Angiology, Hannover Medical School, Hannover, Germany;

[5]Helmholtz Centre for Infection Research, Model Systems for Infection and Immunity, Braunschweig, Germany;

[6]CFPM, FlowCore, Medical Faculty Mannheim of Heidelberg University, Mannheim, Germany;

[7]ECAS, Department of Experimental Pharmacology, Medical Faculty Mannheim of Heidelberg University, Mannheim, Germany;

[8]Institute of Functional and Applied Anatomy, Core Unit Electron Microscopy, Hannover Medical School, Hannover, Germany;

[9]Institute of Molecular and Translational Therapeutic Strategies (IMTTS), Hannover Medical School, Hannover, Germany;

[10]Department of Internal Medicine III, Heidelberg University, Heidelberg, Germany;

[11]ECAS, Cardiovascular Genomics and Epigenomics, Medical Faculty Mannheim of Heidelberg University, Mannheim, Germany.

*these authors contributed equally.

**Address for Correspondence:**
Prof. Dr. Joerg Heineke
Department of Cardiovascular Physiology
European Center for Angioscience (ECAS)
Medical Faculty Mannheim
Heidelberg University
Ludolf-Krehl-Straße 7 – 11
68167 Mannheim, Germany

Phone: +49 621 383 71850
Email: Joerg.Heineke@medma.uni-heidelberg.de

## Abstract

**Background:** Pathological cardiac overload triggers maladaptive myocardial remodeling that predisposes to the development of heart failure. The contribution of long non-coding RNAs (lncRNAs) to intercellular signaling during cardiac remodeling is largely unknown.

**Methods:** We analyzed the expression of *Gadlor 1* and *Gadlor2* lncRNAs in mouse hearts, mouse cardiac cells, extracellular vesicles (EVs), human failing hearts as well as patient serum. *Gadlor* knock-out (KO) mice were generated and analyzed. The effect of *Gadlor* knock-out and *Gadlor* overexpression during cardiac pressure overload induced by transverse aortic constriction (TAC) was analyzed by echocardiography, histological analyses and RNA sequencing in isolated cardiac cells. *Gadlor1/2* interaction partners were identified by RNA antisense purification coupled with mass-spectrometry (RAP-MS).

**Results:** In the heart, the related lncRNAs *Gadlor1* and *2* are mainly expressed in endothelial cells and to a lesser extent in fibroblasts. *Gadlor1/2* are upregulated in failing mouse hearts as well as in the myocardium and in serum of heart failure patients. Interestingly, *Gadlor1* and *2* are secreted from endothelial cells within EVs, which are taken up by cardiomyocytes. *Gadlor*-KO mice exerted reduced cardiomyocyte hypertrophy, diminished myocardial fibrosis and improved cardiac function, but paradoxically suffered from sudden death during prolonged overload. *Gadlor* overexpression, in turn, triggered hypertrophy, fibrosis and cardiac dysfunction. Mechanistically, *Gadlor1* and *Gadlor2* inhibit angiogenic gene expression in endothelial cells, while promoting the expression of pro-fibrotic genes in cardiac fibroblasts. In cardiomyocytes, *Gadlor1/2* upregulate mitochondrial genes, but downregulate angiogenesis genes, while interacting with the transcriptional regulator Glyr1 and the calcium/calmodulin-dependent protein kinase type II (CaMKII), entailing cardiomyocyte hypertrophy and perturbed cardiomyocyte calcium dynamics.

**Conclusions:** We describe that *Gadlor1* and *2*, two related, novel lncRNAs, are upregulated in cardiac pathological overload and are secreted from endothelial cells within EVs. *Gadlor1/2* induce cardiac dysfunction, cardiomyocyte hypertrophy and myocardial fibrosis by exerting heterocellular effects on cardiac cellular gene-expression and by affecting calcium dynamics in cardiomyocytes, which take up the *Gadlor1/2* by EV mediated transfer from endothelial cells. Targeted inhibition of *Gadlor* lncRNA*s* in endothelial cells or fibroblasts might serve as a therapeutic strategy in the future.

## Introduction

Despite recent advances in therapeutic options, chronic heart failure is still one of the leading causes of global mortality, in part due to insufficient means to counteract maladaptive cardiac remodeling.[1-3] Cardiac remodeling comprises global changes in heart shape and function that are the consequence of cardiomyocyte hypertrophy, altered angiogenesis and myocardial fibrosis.[4,5] It leads to ventricular dysfunction, arrhythmia, and consequently heart failure and death.[6,7] The majority of current therapeutic options target protein-coding genes; however, recent studies revealed the significance of non-coding transcripts in cardiovascular development and disease conditions.[5,8,9]

Long non-coding RNAs (lncRNAs) are a diverse group of non-coding transcripts that are longer than 200 nucleotides, and that in general do not encode for proteins.[10] Due to their complex structure, lncRNAs can act, for instance, as chromatin modifiers or microRNA (miRNA) sponges, promote or inhibit protein-protein interactions and thereby affect protein functions, or alter mRNA stability or processing.[5] Thereby lncRNAs typically affect gene expression, alternative splicing or signaling pathways.[11,12] Recent studies have identified lncRNAs with a crucial role in regulating cardiac remodeling via different mechanisms. For instance, the lncRNA *Chast* (cardiac hypertrophy-associated transcript) induces cardiac hypertrophy by disrupting the cardiomyocyte autophagy process via downregulation of *Plekhm1* (Pleckstrin homology domain-containing protein family M member 1), whereas *Mhrt* (myosin heavy-chain-associated RNA transcript) is a cardiac-specific anti-hypertrophic lncRNA that protects against heart failure by directly binding to Brg1 (Brahma-related gene 1) and preventing its chromatin remodeling function.[13,14] Since non-coding transcripts are detectable in human body fluids such as serum/plasma and urine, circulating miRNAs and lncRNAs are currently being investigated as alternative clinical biomarkers, as well as for being paracrine mediators of cellular communication during stress conditions.[15-17]

Intra-myocardial communication is a highly regulated process governing the complex physiology of the heart, whereby proper synchronization is required between cardiomyocytes, endothelial cells (EC) and fibroblasts as the major cardiac cell types.[18,19] Cellular communication during remodeling in response to stress signals can be mediated by secreted proteins, but also by the secretion and transfer of nanoscale extracellular vesicles (microvesicles and exosomes, termed small extracellular vesicles, EVs, in here) that can carry non-coding RNAs and alter the behavior of recipient cells.[20-23] For example, cardiomyocytes, fibroblasts and EC communicate by exchanging miRNAs.[24,25] It is currently emerging that EVs also transport lncRNAs between cells and can thereby affect endothelial cell function and cardiac fibrosis, although not much is known in this regard.[21,23,26]

Here, we identified two related and secreted lncRNAs *Gadlor1* and *Gadlor2* (GATA-downregulated long non-coding RNA), which are markedly upregulated after endothelial deletion of GATA2 (Froese N et al., unpublished observation). We found that the expression of *Gadlor* lncRNAs are significantly increased in mice after transverse aortic constriction (TAC), but also in the myocardium and in serum of patients suffering from chronic heart failure. Moreover, our results revealed that *Gadlor1* and *Gadlor2* are secreted within EVs predominantly by cardiac EC, from which they are mainly taken up by cardiomyocytes, although they also have autocrine/intracrine effects on EC and fibroblasts. In cardiomyocytes, *Gadlor1/2* impact calcium handling and gene-expression, while they trigger pro-fibrotic gene expression in fibroblasts and anti-angiogenic effects in EC. Administration of *Gadlor1/2* containing EVs after TAC exaggerated cardiac dysfunction, augmented fibrosis and cardiomyocyte hypertrophy. Systemic genetic deletion of the *Gadlor1* and *Gadlor2* loci, in turn, led to improved cardiac function, reduced hypertrophy and strongly diminished fibrosis, although increased mortality emerged in *Gadlor* knock-out (KO) mice upon prolonged pressure overload. Our study reveals that secreted *Gadlor* lncRNAs exert heterocellular effects aggravating cardiac remodeling, and that targeted *Gadlor* inhibition in non-myocytes might serve as novel therapeutic strategy in heart failure.

## Results

### Increased expression of *Gadlor* lncRNAs in cardiac pressure overload in mice and in human failing hearts

Previous observations by our group had identified two previously unknown lncRNAs named as GATA-downregulated long non-coding RNA1 and 2 (*Gadlor1* and *Gadlor2*), which were markedly upregulated in EC of endothelial specific GATA2 knock-out mice. *Gadlor1* (AK037972) and *Gadlor2* (AK038629) are located in close proximity to each other on mouse chromosome 16, and are embedded after exon1 of the *Lsamp* (limbic system-associated membrane protein) gene in its intronic region **(Figure 1A, Supp. Figure 1A)**. *Lsamp* is mainly expressed in the brain, and we did not detect significant *Lsamp* expression in the heart or cardiac EC, and *Lsamp* expression also did not change in response to *Gadlor* knock-out **(Supp. Figure 1B)**. *Gadlor1* and *Gadlor2* fragments are not matched with any known mouse peptides (blastp, The National Center for Biotechnology Information (NCBI) database), and we verified that they are non-coding transcripts by using the CPAT algorithm to assess protein-coding probability **(Supp. Figure 1C)**. Cardiac *Gadlor1/2* expression is low in the direct postnatal period, but becomes upregulated in the adult (2 months old) heart **(Figure 1B)**. *Gadlor* lncRNAs are highly conserved between human, mouse and rat **(Figure 1A)**. The degree of conservation between different species were analyzed with the EMBOSS-Water platform by

assessing the local alignment of human and mouse sequences **(Supp. Figure2)**. Cellular expression analysis among the main cell types in the heart revealed the highest *Gadlor1* and *Gadlor2* expression in EC, followed by fibroblasts (FB), while the lowest levels were detected in cardiomyocytes (CM) **(Figure 1C)**. In this analysis, *Gadlor* lncRNA levels were also significantly enriched in EC versus whole heart tissue.

Next, we assessed *Gadlor1/2* RNA levels during cardiac stress and disease. Myocardial *Gadlor1* and *Gadlor2* expression was strongly upregulated in the in the chronic phase (12 weeks) after TAC versus sham hearts **(Figure 1D)**. Importantly, *GADLOR1* and *GADLOR*2 expression was also strongly induced in the myocardium of patients suffering from advanced heart failure **(Figure 1E)**. We developed an assay to measure *GADLOR2* levels in human serum. *GADLOR2* levels were significantly increased in patients with heart failure due to aortic stenosis **(Figure 1F)**. In this patient cohort, high *GADLOR* levels were found mainly in patients with low left ventricular ejection fraction, and a negative correlation between these two parameters was identified **(Figure 1G).**

Taken together, these results demonstrate *Gadlor1* and *Gadlor2* as lncRNAs that are co-upregulated in diseased mouse and human hearts and serum of patients.

### ***Gadlor*** **lncRNAs are enriched in EC-derived extracellular vesicles (EVs)**

Since *GADLOR2* was detectable in serum of heart failure patients, and secreted EVs can contain lncRNAs as shown in previous studies,[21,24] we hypothesized that *Gadlor*1/2 might be secreted within EVs. To test our hypothesis, the abundance of *Gadlor1* and *2* was analyzed in cultured primary mouse cardiac ECs and EVs collected and purified from the supernatant of the ECs by ultracentrifugation **(Supp. Figure 3A)**. Initially, we characterized the isolated EVs with electron microscopy (EM), nanoparticle tracking analysis (NTA) and FACS analysis. We found typical microvesicles and exosomes in EM, and the average size of the particles was slightly larger than 100 nm in diameter by NTA, which showed that they were in the range of microvesicles and exosomes (together called as EVs in this study) **(Supp. Figure 3B-C)**. Flow cytometry assessment also confirms the presence of CD63, CD9 and CD54 as common cell surface markers for EV identification **(Supp. Figure 3D)**.

Interestingly, the absolute concentration of *Gadlor1 and 2* was markedly higher in cardiac EC derived EVs compared to cardiac ECs themselves **(Figure 1H)**. EV *Gadlor1* and *2* RNA levels were not affected by proteinase K (PK), or by RNase A, which indicated *Gadlor1/2* were encapsulated within vesicles and protected from enzyme degradation **(Figure 1I)**. Indeed, *Gadlor* lncRNAs were not protected upon direct incubation with PK and RNase A, or when EVs were dissolved by TritonX, before RNase A was applied

**(Figure 1I)**. In addition to primary cardiac EC, also C166 mouse EC secrete *Gadlor* RNAs in EVs **(Supp. Figure 3E)**. Altogether, these results suggest that *Gadlor1* and *Gadlor2* are highly enriched and encapsulated in EC derived EVs.

### ***Gadlor*-KO mice were protected from cardiac dysfunction during cardiac pressure-overload**

To investigate the role of *Gadlor1* and *Gadlor2*, systemic *Gadlor* knock-out mice (*Gadlor*-KO) were generated by deletion of the whole region of mouse chromosome 16 by using a CRISPR-Cas9 based strategy **(Figure 2A, Supp. Figure 1A)**. Unchallenged *Gadlor*-KO mice were indistinguishable from their wild-type littermates (WT) based on appearance, body weight, heart weight, and baseline echocardiographic analysis **(Supp. Figure 4A-D)**. We detected, however, a mild increase in liver and decrease in brain weight in KO animals compared to WT littermates (**Supp. Figure 4E**).

The ablation of *Gadlor1/2* was confirmed in knock-out animals by qRT-PCR in different organs **(Figure 2B).** We found the highest expression levels of *Gadlor1* and *Gadlor2* in the brain, liver, kidney and as well as in the heart compared to other organs in WT animals **(Figure 2B)**. To study the effect of *Gadlor1* and *Gadlor2* in cardiac remodeling during pressure-overload, WT and *Gadlor*-KO animals were subjected to TAC or sham surgery and subsequently monitored for 2 weeks **(Figure 2C)**. The carotid flow was measured after 2 days of TAC in the right and left common carotid arteries to evaluate the strength of constriction in the aortic arch. The RCCA/LCCA (right to left common carotid) artery flow ratio increased to a similar degree in both WT and *Gadlor*-KO animals, indicating comparable pressure overload **(Supp. Figure 4F-G).** Our results demonstrated a significant increase in heart weight to body weight (HW/BW) ratio after 2 weeks of TAC in both WT and *Gadlor*-KO compared to sham animals, however, less hypertrophy (i.e. a reduced HW/BW ratio) was observed in *Gadlor*-KO mice **(Figure 2D)**. Additionally, heart-failure induced pulmonary congestion was only observed in WT animals after 2 weeks of TAC, whereas *Gadlor*-KO animals were protected **(Figure 2E)**. Cardiac function and dimensions before TAC (pre-TAC) and 2 weeks after the surgery (2w TAC) were recorded by echocardiography with a Vevo 3100 device (Visualsonics-Fujifilm). *Gadlor*-KO mice showed less TAC-induced cardiac systolic dysfunction as manifested by preserved ejection fraction after TAC. Furthermore, *Gadlor*-KO mice exerted a markedly reduced left ventricle wall thickness (LVPW) and less chamber dilation measured as the left end-diastolic volume (LVEDV) compared to WT mice after TAC **(Figure 2F-I)**.

**Deletion of *Gadlor1* and *Gadlor2* alleviates cardiomyocyte hypertrophy and fibrosis *in vivo***

We investigated ultrastructural changes in the myocardium after TAC. Sirius red staining revealed strongly diminished myocardial fibrosis in *Gadlor*-KO mice, which was supported by reduced cardiac *Col1a1* and *Col3a1* mRNA levels after TAC **(Figure 2J-L).** In line with the reduced cardiac hypertrophy at the organ level (i.e., a diminished HW/BW ratio), we confirmed this at the molecular level by reduced expression of *Nppa, Nppb*, a lower *Myh7/Myh6* RNA ratio, and at the cellular level by reduced cardiomyocyte cross-sectional area in *Gadlor*-KO animals after TAC compared to WT littermates **(Figure 2M-O).** Additionally, Isolectin B4 (IB4) staining of capillaries revealed a substantial increase of capillary density in the myocardium of *Gadlor*-KO mice compared to WT animals after TAC **(Figure 2N, P).**

Together, our data showed that deletion of *Gadlor*1/2 protected against cardiac hypertrophy, systolic dysfunction and myocardial fibrosis during cardiac pressure-overload.

**Overexpression of *Gadlor1* and *Gadlor2* via EVs triggers cardiac dysfunction and fibrosis**

In order to decipher the functional effect of increased *Gadlor1* and *Gadlor2* levels during pressure-overload, we administered control EVs and *Gadlor* enriched EVs to mouse hearts directly before TAC surgery by intra-ventricular injection (and concomitant cross-clamping of aorta and pulmonary artery distal of the origin of the coronary vessels). Control EVs were produced by purifying EC derived EVs from the supernatant of control adenovirus (Ad.β*gal*) infected C166 mouse EC, and *Gadlor1* and *Gadlor2* containing EVs were produced by purifying EVs from the supernatant of Ad.*Gadlor1* and Ad.*Gadlor2* infected C166 ECs **(Figure 3A)**. We detected significantly higher levels of myocardial *Gadlor1* and *Gadlor2* after 1 week of the administration **(Figure 3B)**. *Gadlor*-EV treated mice exerted a marked reduction of cardiac systolic function 1 and 2 weeks after TAC, as well as increased wall thickness (indicative of enhanced hypertrophic remodeling), but unchanged left ventricular end-diastolic dimensions (LVEDA) compared to control EV treated animals (indicated as Cohort I and II **Figure 3A-E**). Histological analyses by Sirius red staining showed exaggerated myocardial fibrosis in *Gadlor*-EV treated mice, which was confirmed by qPCR of *Col1a1* and *Col3a1* mRNA expression in the myocardium **(Figure 3G-I)**. Furthermore, increased expression of *Nppa* and *Nppb*, as well as a trend towards larger cardiomyocyte cross-sectional area verified increased hypertrophic remodeling in *Gadlor*-EV treated mice **(Figure 3I-J)**. The myocardial capillary density, however, was not changed between experimental groups **(Figure 3L)**.

We concluded that overexpression of *Gadlor1* and *Gadlor2* via administration of endothelial derived EVs aggravated cardiac dysfunction and hypertrophy, and triggered fibrosis during cardiac pressure-overload.

**_Gadlor_-KO mice exerted increased mortality during chronic pressure-overload**

Next, we studied whether the protective effects of *Gadlor1/2* ablation were maintained during persisting long-term pressure overload, by following WT and *Gadlor*-KO animals for up to 8 weeks after TAC **(Supplement Figure 5A)**. Similar to our findings after 2 weeks of TAC, *Gadlor*-KO animals had a significantly reduced HW/BW ratio after 8-weeks TAC compared to WT littermates, an improved systolic left ventricular function with reduced posterior wall thickness, an increased capillary density, diminished cardiac hypertrophy and markedly less fibrosis **(Supplement Figure 5B-J)**. Despite retaining better systolic function and improved remodeling features, we observed a considerably higher mortality rate in *Gadlor*-KO mice starting between two and three weeks after TAC **(Supplement Figure 5K)**. Interestingly, WT and KO animals were indistinguishable in terms of appearance, behavior and mobility after TAC operation, and death in *Gadlor*-KO mice was unexpected and sudden in nature, possibly due to cardiac arrhythmia.

**_Gadlor1_ and _Gadlor2_ affect gene-expression and angiogenic function in ECs**

Since ECs are the main cardiac cell-type expressing *Gadlor1/2*, and since we observed an increased capillary density in the myocardium of *Gadlor*-KO mice after 2 and 8 weeks of TAC (see above), we performed RNA sequencing from isolated WT and *Gadlor*-KO ECs after 2-weeks of TAC. The purity of EC in our MACS based isolation procedure is >90%.[27] The genome-wide transcriptome analysis via bulk RNAseq identified a total of 3355 differentially expressed (DE) genes between WT and *Gadlor*-KO, which are shown in the heatmap **(Figure 4A)**. Gene ontology analysis from DE genes revealed an upregulation of angiogenesis, mitotic cell-cycle and respiratory electron transport related genes and downregulation of inflammatory response genes in *Gadlor*-KO ECs after 2-weeks TAC **(Figure 4B)**. The upregulation of *Angptl4, Klf15, Aurkb, Cdk1* and the downregulation of *Tlr9, Cxcl2, Icam5, Sirt1* RNAs was confirmed by qRT-PCR in *Gadlor*-KO ECs **(Figure 4C-D)**. Additionally, heart tissue samples were stained with IB4 and Ki67 as a proliferation marker, which revealed higher amount of Ki67 positive ECs in *Gadlor*-KO mice after TAC **(Figure 4E-F)**. As gain of function approach, we overexpressed *Gadlor1* and *Gadlor2* by adenovirus in C166 mouse ECs and performed sprouting assays in comparison to Ad.β*gal* (control) infected cells. FGF2 increased angiogenic sprouting in Ad.β*gal*, but not in *Gadlor1/2* overexpressing cells. Furthermore, TGFβ

decreased sprouting, and this response was enhanced upon adenoviral *Gadlor1/2* overexpression **(Figure 4G-H)**. In summary, *Gadlor* lncRNAs exert anti-angiogenic properties in ECs.

**Cardiac FBs of *Gadlor*-KO mice showed less induction of fibrosis-associated genes after TAC**

Based on our findings, cardiac FBs exerted the second highest *Gadlor* lncRNAs expression after EC **(Figure 1C).** To study FB specific gene-expression changes upon *Gadlor* knock-out, we performed bulk RNAseq from isolated cardiac FBs after 2-weeks TAC. The purity of cardiac FBs in our MACS based isolation procedure is >90%.[27] Genome-wide analysis revealed total of 915 downregulated and 998 upregulated genes in *Gadlor*-KO FBs compared to WT mice after TAC, which are shown in a heatmap in **Figure 5A**. Amongst these, we detected a strong downregulation of mainly ECM organization associated genes (confirmed by RT-qPCR: *Fgfr1, Igf1, Col1a1, Col3a1, Col6a1*) **(Figure 5B-D)**. Additionally, genes related to the regulation of angiogenesis, blood vessel and endothelium development were upregulated in *Gadlor*-KO FBs, which suggested a contribution of FBs for vessel development and angiogenesis observed in *Gadlor*-KO ECs upon overload. The increased expression of *Angpt2, Efna1, Aurkb, Dll1* in cardiac FBs from *Gadlor KO* mice was confirmed by RT-qPCR **(Figure 5C)**. Upon adenoviral overexpression of *Gadlor1* and *Gadlor2* followed with phenylephrine (PE) stimulation, neonatal rat cardiac fibroblasts (NRFB) exerted a decreased expression of *Angpt2*, and an increased expression of *Col1a1* and *Col3a1*, but no differential expression was observed for *Col4a1* or *Col6a1* **(Figure 5E)**.

We concluded that *Gadlor* lncRNAs trigger a pro-fibrotic gene-expression in cardiac FBs.

***Gadlor* lncRNAs are transferred to cardiomyocytes via EC-derived EVs**

Because EC mainly secrete *Gadlor1/2*, we reasoned that these lncRNAs might exert paracrine effects after EV mediated transfer to cardiomyocytes, where they could affect contraction, arrhythmia or hypertrophy. To analyze whether *Gadlor*s are transferred from ECs to cardiomyocytes, we initially overexpressed *Gadlor1/2* (or β*gal* as control) by adenovirus in C166 mouse ECs, and purified EVs from the supernatant of these cells **(Figure 6A)**. We confirmed the enhancement of *Gadlor1/2* expression in EVs upon *Gadlor1/2* overexpression versus control ECs **(Figure 6B)**. The collected EVs were transferred either to neonatal rat cardiomyocytes (NRCMs) or NRFBs. RT-qPCR analysis showed a significantly higher abundance of *Gadlor1/2* in NRCMs incubated with *Gadlor*-EVs compared to samples incubated with control-EVs or cardiomyocytes without any EV treatment, which indicated that EVs were taken up by CMs **(Figure 6C)**.

*Gadlor* lncRNAs were also transferred from ECs to cardiomyocytes by control EVs, since higher cardiomyocyte *Gadlor1/2* levels were observed after control EV compared to non-EV treatment. Additionally, a mild increase in both *Gadlor1* and *Gadlor2* abundance was also observed in NRFBs after incubation with *Gadlor* EVs, however, at a much lower degree compared to NRCM **(Figure 6C)**. We visualized the uptake of the fluorescently-labelled (PKH67) EVs into recipient cardiomyocytes, which was analyzed with confocal microscopy after 6 hours and 24 hours **(Figure 6D)**. 3D imaging by confocal Z-stacks confirmed that EVs were internalized into the recipient cardiomyocytes rather than being attached on the surface **(Supplement Video 1)**.

Furthermore, we conducted experiments with isolated *Gadlor*-KO CMs (lacking endogenous *Gadlor1/2* expression) in co-culture with mouse cardiac endothelial cells (MCEC, on cell culture inserts) for 48 hours **(Figure 6E)**. *Gadlor*-KO cardiomyocytes were used to exclude confounding effects of endogenous *Gadlor1/2* expression with exogenous *Gadlor1/2* uptake from EC derived EVs. As expected, we did not detect any *Gadlor1/2* expression in isolated *Gadlor*-KO CMs when they were kept in monoculture, whereas we detected *Gadlor1* and *Gadlor2* after co-culture with MCECs **(Figure 6F)**. These results suggested that *Gadlor1/2* were transferred into *Gadlor*-KO CMs from MCECs via EV-mediated cell-to-cell transfer. Notably, MCECs that were co-cultured with *Gadlor*-KO CMs were also increasing their expression of *Gadlor*1/2 **(Figure 6F)**, which might suggest a possible feedback mechanism between CMs and ECs. Next, we performed sub-cellular fractionation to localize *Gadlor* lncRNAs after their uptake by the recipient NRCMs. *Gadlor1* and *Gadlor2* expression was detected in the cytosol and in a bit higher levels in the nucleus of recipient cardiomyocytes **(Figure 6G)**. Overall, these results suggested that endothelial-derived *Gadlor1/2* containing EVs are mainly taken up by cardiomyocytes, where they might act in the cytosol as well as in the nucleus. Cardiac FBs may mainly rely on their own cellular *Gadlor1/2* expression.

### ***Gadlor* lncRNAs bind to calcium/calmodulin-dependent protein kinase type II - subunit delta in cardiomyocytes**

LncRNAs can interact with proteins to affect their regulatory functions[28]. Even though CMs showed the least endogenous levels of *Gadlor* lncRNAs, we still observed a strong effect in cardiomyocytes after *Gadlor1/2* deletion upon pressure overload. To decipher this further, we aimed at identifying the binding partners of *Gadlor1/2* in cardiomyocytes by performing RNA antisense purification coupled with mass-spectrometry (RAP-MS) in HL1 cardiac muscle cells after overexpression of *Gadlor1/2*. Interestingly, we found calcium/calmodulin-dependent protein kinase type II, subunit delta (CaMKIIδ) as well as the gene-

regulatory factor GLYR1 a significant binding partner of *Gadlor1/2* **(Figure 7A)**. Next, we validated the interaction of CaMKII and GLYR1 with *Gadlor1/2* with native RNA immunoprecipitation (RIP) followed by qRT-PCR, which showed a significant enrichment of *Gadlor1* and *Gadlor2* after CaMKII and GLYR1 IPs versus IP with IgG control **(Figure 7B-C)**. Moreover, we also identified reduced and increased phospholamban phosphorylation at the Thr17 direct CaMKII phosphorylation site in *Gadlor*-KO mice or *Gadlor*-EV treated mice after TAC, respectively **(Figure 7D-G)**. This indicated that *Gadlor1/2* might promote CaMKII activation in cardiomyocytes.

Because we had identified an impact of *Gadlor* lncRNAs on cardiac function, and because we identified CaMKII as binding partner, which has a known role in cardiomyocyte excitation-contraction coupling, we investigated cardiomyocyte contractility and calcium dynamics with the Multicell HT system (Ionoptix) in isolated adult cardiomyocytes after 1-week of TAC. Interestingly, the analysis software detected considerably high number of *Gadlor*-KO cardiomyocytes with arrhythmic behavior during the measurements compare to WT CMs **(Figure 7H)**. Additionally, while sarcomere shortening and the timing of shortening was not affected, the timing of cardiomyocyte relaxation was delayed **(Figure 7I-J)**. Interestingly, *Gadlor*-KO CMs displayed a much slower re-uptake of calcium into the sarcoplasmic reticulum (SR), which led to prolonged calcium transients and also an increased calcium peak height in *Gadlor*-KO cardiomyocytes **(Figure 7K-L).** Treatment of adult mouse cardiomyocytes with *Gadlor1/2* enriched EVs, versus control EC derived EVs led to augmented, but slower sarcomere shortening, and especially faster cardiomyocyte relaxation **(Figure 7M)**. While calcium peak height and calcium release time were not changed, a faster diastolic calcium re-uptake was detected by a decreased tau value **(Figure 7N)**. Collectively, *Gadlor*-KO myocytes exerted enhanced arrhythmic beating, slower diastolic relaxation and calcium re-uptake into SR which entailed as increased intercellular calcium levels. Overexpression of *Gadlors1/2* in turn, led to faster cardiomyocyte relaxation and faster re-uptake of calcium into the SR.

### ***Gadlor1* and *Gadlor2* affect cardiomyocyte gene expression**

Since *Gadlor*1/2 were in part localized in the cardiomyocyte nucleus after transfer, we hypothesized that they might also have a role in regulation of the gene expression in these cells. To investigate this, we performed bulk RNA sequencing from isolated adult cardiomyocytes of WT and *Gadlor*-KO after 2-weeks TAC. Comprehensive transcriptome analysis after TAC between WT and *Gadlor*-KO revealed that 2492 genes were upregulated, while 2956 genes were downregulated after ablation of *Gadlor1/2* as shown in the heatmap in **Figure 8A**. Functional annotation of differentially expressed genes showed that genes

related to vasculature development, ECM organization and regulation of cytokine production were upregulated **(Figure 8B)**, while mitochondrial organization, TCA cycle and cardiac muscle contraction associated genes were significantly downregulated in *Gadlor*-KO mice compared to WT after 2-weeks TAC **(Figure 8B)**. We confirmed the upregulation of *Il6, Tlr9, Col15a1, Col14a1, Adam8* RNAs, and the downregulation of *Camk2d, Gata4, Actn2, Mfn2* RNAs in Gadlor-KO cardiomyocytes after TAC by RT-qPCR **(Figure 8C-D)**. To rule out a reduced number of mitochondria as reason for the downregulation of mitochondrial genes, we assessed the mitochondrial to nuclear DNA ratio, but detected no changes in *Gadlor*-KO versus WT mice **(Figure 8E)**. We next assessed the effects of *Gadlor1/2* overexpression in cardiomyocytes after PE stimulation. We found an upregulation (or a tendency towards upregulation) of *Gata4, Cox5a, Mfn2* and *Rcan1.4* RNAs, and a downregulation (or a tendency towards downregulation), for *Angpt2* and *Klf15* RNAs upon *Gadlor1/2* overexpression **(Figure 8F)**. This showed that *Gadlor1/2* overexpression in large parts revealed the opposite effects of what was found in *Gadlor*-KO cardiomyocytes.

Comparing the effects of *Gadlor* knock-out in the different cardiac cell types after TAC, revealed a strong overlap among upregulated and downregulated genes in FBs, ECs and cardiomyocytes **(Supplemental Figure 6)**. For example, *Gadlor* knock-out led to the upregulation of energy coupled proton transport mitochondrial genes, actin filament associated genes, and mitotic cell cycle related genes in all three cell types, in addition the upregulation of cardiac muscle contraction and blood vessel morphogenesis genes in two cell types. On the other hand, genes related to the negative regulation of cell differentiation, cartilage development and the regulation of membrane potential were downregulated in all three cell types, while genes related to cell migration, to the inflammatory response, to extracellular matrix organization, to heart contraction, to calcineurin/NFAT signaling and to mitochondrial organization were downregulated in at least two of the cell types **(Supplemental Figure 6)**. Therefore, *Gadlor1/2* effects on gene-expression contain common, but also unique targets in different cardiac cell types. An overview of our findings is given in **Supplemental Figure 7**.

## Discussion

Here, we describe two novel, related lncRNAs (termed *Gadlor1* and *Gadlor2*) as central regulators of cardiac failure during pressure overload. *Gadlor1* and *Gadlor2* were upregulated in mouse and human failing hearts as well as in serum of patients with aortic stenosis, where high *GADLOR2* levels were associated with a low ejection fraction. Accordingly, enhanced experimental *Gadlor1/2* expression in

mouse hearts triggered aggravated heart failure, myocardial hypertrophy and fibrosis, while combined *Gadlor* knock-out mice were protected from cardiac dysfunction, fibrosis and vascular rarefaction during acute and persisting pressure overload. Paradoxically, despite retaining better heart function, the complete lack of *Gadlor* lncRNAs during chronic, persisting pressure overload entailed sudden death, most likely due to arrhythmia.

Among the different cell types in the myocardium, we found the highest *Gadlor1/2* expression in ECs, where reduced *Gadlor1/2* levels entailed an increased capillary density and increased endothelial cell proliferation after TAC. *Gadlor1/2* overexpression in isolated ECs, in turn, reduced angiogenic activity, indicating that *Gadlor* lncRNAs inhibits angiogenic activity in EC in a cell autonomous manner. The fact that we did not observe a reduced myocardial capillary density after TAC upon *Gadlor* overexpression might be due to insufficient overexpression of *Gadlor* containing extracellular vesicles in EC. Because lncRNAs often exert their effects by modifying gene-expression, we performed transcription profiling by RNA sequencing in cardiac EC after TAC. Indeed, we found that upon *Gadlor*1/2 deletion, EC upregulate genes related to angiogenesis and cell cycle and mitosis, while at the same time downregulating pro-inflammatory genes. Beside this cell autonomous role, *Gadlor*-KO mice also exerted an increased expression of proangiogenic genes in cardiomyocytes and FBs during TAC, which are known to affect angiogenesis in a paracrine manner.[29-32]

In addition to EC, cardiac FB exerted a rather high *Gadlor1/2* expression in the heart, while expression was low in cardiomyocytes. Transcriptomic profiling in cardiac FBs showed an enhanced expression of angiogenesis related genes, suggesting a paracrine effect on EC as mentioned above. More importantly, it revealed the downregulation of many extracellular matrix-organizing genes, including pro-fibrotic growth factors, their receptors as well as matrix proteins themselves (e.g. *Col1a1* and *Col6a1*). Combined adenoviral overexpression of *Gadlor1* and *Gadlor2* in isolated rat cardiac FBs upon phenylephrine stimulation triggered the opposite effect (i.e. downregulation of angiogenesis genes and upregulation of matrix genes) for some, but not all of the genes identified by RNA-seq. These data imply that the pro-fibrotic role of *Gadlor1* and *Gadlor2* are mediated by their direct effect on gene-expression in cardiac FBs.

Remarkably, *Gadlor1/2* are mainly secreted within EVs from EC, which was indicated by a highly enriched *Gadlor* expression in endothelial derived EVs versus EC. This finding indicated a potential paracrine role of *Gadlor* lncRNAs in the heart. Indeed, EVs were reported to contain mainly miRNAs, but also lncRNAs and mRNAs and to protect these RNA species from degradation by extracellular RNases.[33] EVs might thereby play a role in intercellular communication, especially during stress stimulation or

disease, when their production is typically upregulated.[34] In cell culture experiments, we found an effective uptake of *Gadlor1/2* from endothelial derived EVs in neonatal and adult cardiomyocytes. When adult cardiomyocytes from *Gadlor*-KO mice that naturally could not upregulate intrinsic *Gadlor1/2* lncRNA expression were co-cultured in the bottom well of a two-chamber system with wild-type EC in the upper well, these effectively restored *Gadlor1/2* levels in the knock-out cardiomyocytes. In addition, the co-cultured EC markedly upregulated their *Gadlor1/2* expression compared to when they were cultured alone. Although we cannot prove this yet in vivo in the heart, our results nevertheless indicated a reciprocal intercellular signaling circuit between EC and cardiomyocytes, whereby EC provide *Gadlor* lncRNAs within EVs to cardiomyocytes, which signal back to EC by currently unknown mechanisms to indicate insufficient *Gadlor1/2* levels, when necessary. Indeed, signal responsive EV release had been previously described.[34]

In cardiomyocytes, *Gadlor1/2* lncRNAs are taken up from ECs localize to the cytosolic as well as to the nuclear compartment. Accordingly, as *Gadlor*1/2 binding partners, we identified CaMKII, which is present in the cytosol and in the nucleus as well as GLYR1, which has a predominant nuclear localization. GLYR1 was recently identified as nucleosome-destabilizing factor that is recruited to gene bodies to facilitate the transcription of many genes.[35] Thus, *Gadlor1/2* might act on gene-expression in part by binding to GLYR1. CaMKII is activated mainly by calcium/calmodulin, autophosphorylation and oxidation or S-nitrosylation.[36] Its activity is known to be about 3-fold upregulated in failing human hearts.[37] In cardiomyocytes, CaMKII promotes on one hand maladaptive features such as cardiomyocyte hypertrophy and fibrosis by phosphorylating HDAC4, leading to de-repression of MEF2-dependent, pro-hypertrophic gene-expression.[38,39] On the other hand, it has adaptive functions, for example, it promotes calcium re-uptake into the SR by phosphorylating phospholamban at Threonine-17 (Thr17).[40-42] Because *Gadlor1/2* bind CaMKII and *Gadlor*-KO mice exerted a reduced Thr17 phosphorylation, while *Gadlor*1/2 overexpression led to enhanced Thr17 phosphorylation, we concluded that the *Gadlor* lncRNAs might promote CaMKII activation in a feed-forward loop in cardiomyocytes during pathological overload. Indeed, decreased CaMKII activity could account for the improved cardiac remodeling features that we detected in *Gadlor* knock-out mice, while at the same time slowing down calcium re-uptake into the SR, leading to increased cytosolic calcium levels with pro-arrhythmic activity. With regard to their dichotomous role in cardiomyocytes, *Gadlor1/2* inhibition in cardiomyocytes might not be a suitable therapeutic strategy during cardiac overload, since although it would lead to inhibition of hypertrophy, there might be the danger of arrhythmia or sudden death. On the contrary, inhibition of *Gadlor1/2* in EC and FB could be beneficial, as it would entail increased angiogenesis and reduce FB mediated fibrosis,

which according to our data is likely the main underlying reason for *Gadlor1/2* triggered cardiac dysfunction. Although more work is needed, we suggest that the inhibition of *Gadlor* lncRNAs in cardiac non-myocytes might be a promising strategy to treat heart failure in the future.

## Methods

### Human Tissue and Serum Samples

Studies on human heart tissue samples were approved by the Institutional Ethical Board of Massachusetts General Hospital (US). Human heart tissue samples were collected from patients with end-stage heart failure undergoing cardiac transplantation. Control heart tissue samples was obtained from healthy organ volunteers when the organ was not eligible for transplantation, or from the victims of traffic accidents. Human serum samples were obtained from healthy blood donors, or from aortic stenosis patients before replacement of the aortic valve, where all donors were provided a written informed consent for the collection and use of samples, that had received approval from Institutional Review Board of Christian-Albrechts-Universität Kiel (File number: A174/09).

### Measurement of GADLORs in Human Serum Samples

Human serum samples were collected on a day before Transcatheter Aortic Valve Implantation (TAVI). Serum-RNA was extracted using miRNeasy serum/plasma kit (#217184; Qiagen) based on manufacturer's instructions. LncRNA levels were normalized by the addition of 2 µl of TATAA universal RNA Spike (#RS10SII; Tataa Biocenter) prior to RNA-isolation. RNA was transcribed to cDNA (#K1652; Maxima H Minus First Strand cDNA Synthesis Kit; Thermo Fisher) and analyzed with TaqMan Non-coding RNA Technology (#4369016) using custom specific TaqMan Gene Expression Assay (#43331348, ID: APPRKET und APRWEYP; Thermo Fisher). For quantitative RT-PCR, the Stratagene's MX4000 multiplex qPCR system was used.

### Animal Use and Experiments

All studies including the use and care of animals were performed ethically with the permission of the Regional Council Karlsruhe and the Lower Saxony State Office for Consumer Protection and Food Safety, Germany approved protocols 35-9185.81/G-144/18, I-22/03, 33.9-42502-12-10/0016, 33.19-42502-04-14/1403 and 33.8-42502-04-16/2356). All the experiments for the surgical interventions and the following physiological assessments were performed in accord with the terms of informed consents.

Wildtype ICR/CD1 mice were in-bred in- house and C57BL/6N mice were obtained from Janvier Labs (Le Genest-Saint-Isle, France). Animals were maintained in the temperature-humidity controlled (22± 2°C and 35-60% humidity), 12-h dark-light cycled room with unlimited access to water and standard food.

Systemic *Gadlor* knock-out mice (*Gadlor*-KO) were generated by deletion of the whole region of mouse chromosome 16 using a CRISPR-Cas9 based strategy. Briefly, embryonic stem cells (G4 line, doi 10.1073/pnas.0609277104) were transfected with gRNAs LNC1-01 (target sequence: 5'-

TTGTACATGAGCGGTTGTAG) and LNC2-01 (target sequence 5'-AGTATACAGGGGGTTACCAT) as well as in vitro transcribed CAS9-GFP mRNA. GFP expressing cells were sorted and single cell derived clones were established. 5 out of 72 analyzed clones showed extensive deletions between the gRNA target sites. Clone 1-37 comprised a deletion of 39995533 – 40004426 on one chromosome 16 allele. This clone was injected into C57BL/6 blastocysts to generate a transgenic mouse line which was then further crossed to achieve a homozygous deletion. The genotyping primers used listed in the **Supplemental Table 1**.

**Transverse Aortic Constriction (TAC)**

Transverse aortic constriction (TAC) was induced in 8-10 weeks old mice and maintained for 1-week or 2-weeks for short-term and 8-12 weeks for long-term studies. Analgesia (0.1 mg/kg buprenorphine) was provided by subcutaneous injection. Tracheal intubation was followed by upper thoracotomy to visualize the aortic arch, which was tied with a 7-0 silk ligature around a 26-gauge needle that was removed immediately after secured constriction. Mice were injected with 0.1 mg/kg atropine, and the chest wall was closed with suture then followed with closure of skin with surgical glue. The mice were ventilated with 2% isoflurane throughout the procedure. For postoperative care, additional analgesia was provided in drinking water for the following 5 days. To assess the mortality rate, mice were followed and inspected daily after TAC. Sham operated animals were treated with the same procedure and medications, but no constriction was applied to aortic arch.

**Transthoracic Echocardiography**

Echocardiography was performed with 1% isoflurane anesthesia. Mice were dorsally placed on a heated table to maintain the body temperature during the procedure while the ECG and the respiration rate were recorded continuously. Echocardiography was recorded with a linear 30-40 MHz transducer (MX-550D) and the Vevo 3100 system (Visualsonics, Toronto, Canada). Data were analyzed with the VevoLab 5.5.0 software.

***Left Ventricle and Apical four Chamber View.*** Parameters were recorded in B-mode and M-mode in both parasternal long axis (PSLAX) and short-axis (SAX) view at the papillary muscle level. Left-ventricular posterior wall thickness and left-ventricular end-diastolic volume were used to characterize LV microanatomy (LVPW and LVEDV) and the change of LV diameter length from end-diastole (LVID) to end-systole was used to assess contractility and to calculate LV ejection fraction and fractional shortening (LV-EF and LV-FS), which were measured with the PSLAX mode in the analysis. B-mode tracing in the apical four-chamber view was recorded at the atrioventricular valve level with pulse wave-Doppler (PW-Doppler) and tissue-Doppler measurements.

***Carotid flow measurement.*** To evaluate the degree of aortic constriction during TAC surgery, the peak velocity of flow in the right and left common carotid arteries (RCCA and LCCA) were measured 2 days after surgery with PW-Doppler at the level of carotid bifurcation to calculate the ratio of RCCA/LCCA.

**Organ Harvest**

At the end of the experiment, mice were weighed and euthanized to collect the heart, lungs and liver. Organs were washed in cold PBS to remove the blood, and additionally the heart was washed in 0.5% (w/v) KCl in PBS. The heart was transversely cut into half, and upper layer was immediately embedded into OCT for histological analysis while other sections dissected and snap-frozen.

**Histology**

OCT embedded organs were sectioned into slices of 7 µm and 12 µm for immunofluorescence and Picro-Sirius red staining, respectively. Briefly, for immunofluorescence tissue sections were fixed with 4% PFA followed by permeabilization with 0.3% Triton-X in PBS, and blocking with 3% BSA. Primary and secondary antibodies that were used are listed in **Supplemental Table 2**. Samples were visualized with Leica DMi8 Fluorescence microscope. Images were analyzed with Leica Application Suite X (LAS X) 3.7.

Sirius red staining was performed by fixing the tissue samples with 100% ice-cold acetone, and by following the standard protocols. Tissue sections were scanned with Zeiss Axio Scan.Z1. Images were analyzed with ZEN 2.6 Blue Edition, Carl Zeiss.

**Isolation and Culture of Juvenile Mouse Endothelial Cells (mECs)**

Hearts from 7-12 days old mice were collected and washed in ice-cold DMEM high-glucose to clean and remove the atria. The minced tissue was transferred into 5 ml of enzyme solution (for 3-4 hearts) and incubated with collagenase I (500 U/ml, Worthington - LS004176) and DNase I (150 U/ml, Worthington - LS002139) in HBSS (without Ca and Mg). After digestion, the lysate was washed with FCS and passed through a 0.70 µm cell strainer. Washed lysate was incubated with CD31 antibody (BD, 553370) coupled to Dynabeads (Invitrogen, 11035) for the first step of isolation, before the cells were plated on 0.5% gelatinized plates. For culturing, cells were maintained for 3-4 days until they reached 80-90% confluency. During the first passage, further purification of cells was achieved by incubation with CD102 antibody (BD, 553370) coupled Dynabeads. Primary endothelial cells were maintained in DMEM with 20% FCS supplemented with non-essential amino-acids and sodium pyruvate, and passaged up to P3 for experiments.

**Isolation of Adult Mouse Endothelial Cells, Fibroblasts and Cardiomyocytes**

Isolation of endothelial cells and fibroblasts from adult mouse heart was performed with MACS-magnetic beads from Miltenyi Biotec. Briefly, heart tissue was washed in ice-cold PBS, minced into small pieces before incubating in enzyme solution (collagenase I (500 U/ml, Worthington - LS004176) and DNase I (150 U/ml, Worthington - LS002139) in RPMI 1640 (Thermo Fischer Scientific: 31870025)). Digested tissue samples were passed through a 0.70 µm cell strainer and washed with FCS, and MACS buffer with BSA (Miltenyi Biotec, 130-091-222). After multiple washing steps, the tissue lysate was incubated with CD146 microbeads (Miltenyi Biotec, 130-092-007) before being passed through magnetic columns (Miltenyi Biotec, MS columns 130-042-201) for positive selection of endothelial cells (EC). The flow through was incubated with feeder removal microbeads (Miltenyi Biotech, 130-095-531) and eluted after multiple washing steps to collect fibroblasts (FB). Isolated cells were stored as frozen cell pellet for later RNA or

protein isolation for corresponding experiments.

Isolation of adult cardiac myocytes was achieved by using a Langendorff perfusion system.[43] Briefly, immediately after excision, the heart was placed into ice-cold 1x perfusion buffer (10x stock: 1130 mM NaCl ,47 mM KCl, 6mM $KH_2PO_4$, 6 mM $Na_2HPO_4$, 12 mM $MgSO_4.7H_2O$, 120 mM $NaHCO_3$, 100 mM $KHCO_3$, 100 mM HEPES buffer solution and 300 mM Taurine) to clean the tissue around the aorta under a microscope. Then the aorta was placed onto a cannula (inner diameter 1mm) with forceps and tied with silk suture to allow perfusion through the coronary arteries. Subsequently, the heart was perfused with enzyme solution containing Liberase DH (5 mg/ml, Roche, 5401089001), trypsin (1%, Gibco, 15090046) and $CaCl_2$ (100 mM) to digest the tissue at 37°C. Enzymatic digestion was ended with Stop I and II solutions containing perfusion buffer with FCS and $CaCl_2$ (10 mM). Digested heart tissue samples were passed through a 100 µm cell strainer. Then, calcium concentration was gradually increased by manual administration into digested heart tissue with continuous gently mixing. Then the cells were subjected to either IonOptix analysis, culturing or direct RNA and protein extraction (after cardiomyocyte sedimentation).

**Isolation of Neonatal Rat Cardiomyocytes (NRCMs)**

Hearts from 1-3 days old rats were collected and washed with ice-cold 1x ADS (pH 7.35) to clean the blood and remove the atria. The ventricular parts were minced in 1x ADS and digested in enzyme solution containing collagenase Type II (Worthington: LS004176) and pancreatin (Sigma P3292). The resulting cells were loaded onto a Percoll gradient to separate cardiomyocytes (CM) and non-cardiomyocytes. NRCMs were plated ($4.0\times10^5$ /well for 6 well-plate) on 0.5% gelatin coated plates.

**Isolation of Extracellular Vesicles (EVs)**

Isolation of EVs were performed with ultracentrifugation from the supernatant of C166 cells that were cultured with EV depleted FCS. Initially, cell debris and large vesicles (apoptotic bodies) were removed by centrifugations at 300xg and 10.000xg, respectively. Subsequently, small EVs (including microvesicles and exosomes) were collected with 100.000xg ultracentrifugation for 90 minutes, and similarly washed with PBS, before a second round of centrifugation was performed. The EV pellet was re-suspended in PBS for NTA (ZetaView Nanoparticle Tracing Videomicroscope, PMX-120) measurements, or with QIAzol lysis buffer (Qiagen, 79306) for RNA isolation.

***EV-RNA isolation.*** RNA isolation from EVs was performed by RNA precipitation as described before.[44] Briefly, the EV pellet was resuspended with 1 ml of QIAzol, and then mixed with 200 µl of chloroform for phase separation. Samples were mixed thoroughly and incubated for 5 minutes in room temperature (RT), then centrifuged at 12.000xg at 4°C for 15 minutes. The aqueous upper layer was mixed with 10% (v/v) sodium acetate (3M, pH 5.5) and 4 µl of glycogen (5 mg/ml) in 1.5 ml ethanol (100%). Samples were incubated at -80°C overnight, then centrifuged at 16.000xg for 30 minutes to pellet the RNA. The RNA pellet was then washed with 70% ethanol and dried, before being re-suspended in nuclease-free water.

***EV RNase and Proteinase-K Protection Assay.*** To test the transfer of *Gadlor* lncRNAs within EVs, we performed RNase and proteinase K protection assays with and without prior application of Triton-X. in brief, EVs were isolated and treated with 100 ng/µl of RNase A, and 20 mg/µl of proteinase K for 30 minutes at 37°C. 5mM of PMSF was used to inactivate the proteinase K at RT. To disrupt the lipid bilayer, EVs were

incubated with 1% Triton-X for 1 hour for selected samples. As a negative control, RNA isolated from EVs were also treated with the same protocol.

***EV-labelling with PKH67 cell linker.*** To visualize EVs for transfer and re-uptake experiments *in vitro,* they were labelled with PHK67 Green Fluorescent Cell Linker kit (Sigma MIDI67). Briefly, EV pellet was re-suspended with 1 ml of diluent C including 4 µl of PKH67 dye, and incubated for 5 minutes at RT. Then 1% BSA-PBS was added into the suspension to remove the unspecific binding of the dye. Then EVs were pelleted at 3000xg for 1 hour, which were then suspended with the cell culture medium and added on neonatal rat cardiomyocytes. Visualization of EVs was conducted with the Leica Confocal Microscope TCS SP8 and images were analyzed by Leica Application Suite X (LAS X) 3.7.

***EV FACS Staining.*** Characterization of surface markers of EVs was performed with flow cytometry by staining EC-derived EVs with CD9-PerCP-Cy5.5 (Miltenyi Biotec, 130-102-278, Clone: MZ3), CD63-APC (Miltenyi Biotec, 130-108-894, Clone: REA563) and CD54-FITC (BD, 553252, Clone: 3E2) labelled antibodies for 1 hour at 4°C. Measurements were obtained with BD FACSCanto ll.

***EV Transmission Electron Microscopy (TEM).*** Visualization of EVs were performed with TEM. After centrifugation, pellets were resuspended in the minimum possible volume of residual liquid and 25 % aqueous glutaraldehyde was added to a final concentration of 1 %. After fixation overnight, samples were mixed 1:1 (v/v) with 4 % agar at 40 °C. After hardening, the agar blocks were cut to cubes of 1 mm size. Further preparation of samples and electron microscopy were performed as described, before being imaged with a FEI Morgagni 268 transmission electron microscope (FEI, Eindhoven, Netherlands) operated at 80 kV using a Veleta CCD camera (Olympus Soft Imaging Solutions).[45]

**Cell Culture**

C166 (CRL-2581, ATCC) mouse embryonic endothelial cell line and NIH3T3 (CRL-1658, ATCC) mouse fibroblast cell line were cultured in Dulbecco's Modified Eagle's Medium (DMEM) with 10% FCS, while MCECs (CLU510-P, Tebu-bio), immortalized mouse cardiac endothelial cells, were cultured with 5% FCS containing DMEM supplemented with L-glutamine (1%), penicillin/ streptomycin (1%) and HEPES. HL-1 cardiac muscle cells (SCC065, Merck) were cultured with Claycomb media (Sigma, 51800C) supplemented with 10% FCS, 0.1 mM norepinephrine, 2 mM L-glutamine and 1X penicillin-streptomycin (P/S). HL-1 cells were plated on 0.1% gelatin coated flasks, and cell culture media was refreshed daily. Cells were cultured for up to 10 passages.

***Adenoviral infection.*** For overexpression of *Gadlor* lncRNAs, recombinant adenoviruses were used. Mouse cDNAs of AK037972 (*Gadlor*1) and AK038629 (*Gadlor*2) were subcloned into the pShuttleCMV vector (Source Bioscience, UK) and adenoviruses were generated by the AdEasy Adenoviral Vector system (Agilent, 240009). An adenovirus overexpressing β-Galactosidase (Ad*ßgal*) was used as control. After production of adenoviruses, the viral titer was calculated with the help of the AdEasy Viral Titer Kit (Agilent, 972500), and all the experiments were performed with 50 MOI. Adenoviral infection on cultured cells was performed for 4 hours at 37°C on cells with media containing heat-inactivated FCS.

***Co-culture experiments.*** For co-culture experiments, adult mouse cardiomyocytes isolated from *Gadlor*-KO mice were seeded on laminin (Santa Cruz, SC-29012) coated 6-well plates and cultured with MCECs

plated on 1 µm pore-sized inserts (Thincert, Greiner, 657610). Cells were collected separately after 48 hours for RNA isolation.

**Endothelial-cell Sprouting Assay**

To study the effect of *Gadlor* lncRNAs in angiogenesis, we performed sprouting assays with C166 mouse ECs according to a well-established protocol previously described.[46] Briefly, cells were infected with *Ad. ßgal or Ad.Gadlor1/2* adenovirus for 24 hours. 50.000 cells were re-suspended with 4 mL DMEM + 10 % FCS and 1 mL methylcellulose solution (Sigma-Aldrich, M0512) and drops containing 25 µl of suspension were pipetted onto a 10 cm cell culture dish. The drops were then incubated upside-down in a cell culture incubator for 24 hours to allow spheroid formation. On the follwing day, the cell spheroids were collected by gently washing off the hanging drops with PBS and collected by 200xg centrifugation for 5 minutes and re-suspended with methylcellulose solution containing 20 % FCS. Collagen matrix was prepared in parallel on ice with collagen stock solution (Corning, 11563550), diluted in 10x M199 medium (Sigma-Aldrich, M0650) and the required amount of sodium hydroxide to set the pH for polymerization. Then the collagen medium was mixed into spheroids in the methylcellulose solution. 1 mL of the spheroid-collagen-methylcellulose solution were added per well in a 24-well plate and incubated in a cell culture incubator for 30 min to induce the polymerization of the collagen-methylcellulose matrix. The endothelial spheroids were stimulated with 100 µl of DMEM + 10 % FCS, 25 ng/mL FGF2 or 10 ng/mL TGF-β1 by adding it dropwise to the collagen matrix. After 24 hours, the sprouting assay was stopped by adding 1 mL of 4% paraformaldehyde to the wells. Spheroids were visualized with the 10X objective of the bright-field microscopy and analyzed with ImageJ.

**RNA Isolation and qRT-PCR**

RNA isolation from tissue samples was performed with QIAzol reagent (Qiagen, 79306), and from isolated cells with NucleoSpin RNA isolation kit (Macherey-Nagel, 740955.250) according to manufacturers' protocols. cDNA was generated by using the Maxima H minus First stand cDNA synthesis kit (Thermo Fisher Scientific, K1652). Quantitative PCR was performed with the Maxima SYBR Green mix with ROX as reference dye (Thermo Scientific, K0253) on an AriaMx Real-time PCR System (Agilent, G8830a). Gene expression was normalized to *Gapdh*,18S or *U6* expression. All qPCR primer sequences are listed in the **Supplemental Table 3**.

**Protein Isolation and Western blotting**

Heart tissue protein lysates were prepared from frozen pulverized tissue with lysis buffer containing 30 mM Tris-pH 8.8, 5 mM EDTA-pH 8.0, 3% SDS (v/v), 10% glycerol (m/v), protease and phosphatase inhibitors. Protein quantification was performed by BCA assay (ThermoFisher, Pierce BCA Protein Assay kit, 23225). Samples were incubated at 95°C for 5 minutes after addition of Laemmli buffer (1X final concentration) and proteins were separated with SDS-PAGE electrophoresis. The following primary antibodies were used: Calsequestrin (Thermo Scientific PA1-913, rabbit), Phospholamban, pThr17 (Badrilla A010-13, rabbit), Phospholamban (Badrilla, A010-14 mouse). The following secondary antibodies were used: Rabbit anti-mouse peroxidase (Sigma-Aldrich), goat anti-rabbit peroxidase (Sigma-Aldrich).

**Sarcomere Contractility and Calcium Transient Measurements**

Adult cardiomyocytes were isolated 1-week after TAC operation. Cardiomyocytes were plated on laminin coated (10 µg/cm$^2$) 35 mm dishes (MatTek 10 mm Glass bottom dishes, P35G-1.5-10-C) and gently washed 1 hour later with MEM medium without butanedione monoxime (BDM). The plated cells were then transferred into the Ion-Optix Multicell High-throughput System chamber, where they were simultaneously paced (15 V, 3 Hz, 4 ms impulse duration), and assessed for sarcomere length and contraction. Calcium handling was recorded after incubation with 1 µM fura-2, AM (Invitrogen, F1221). After performing the baseline measurements, the cells were perfused with 100 nM isoprenaline for follow-up measurements. The recordings were analyzed with IonWizard software.

**RNA antisense purification coupled with mass spectrometry (RAP-MS)**

To identify the protein interaction partners of *Gadlor* lncRNAs we performed RAP-MS as described previously with minor modifications.[47] The 5' biotinylated antisense *Gadlor1* and *Gadlor2* probes were pooled in the experiment and the sequences are listed in **Supplemental Table 4**. We used HL-1 cardiomyocytes overexpressing *Gadlor1* and *Gadlor2* after infection with Ad.Gadlor1 and Ad.Gadlor2. RNA antisense purification (RAP) was performed with cells collected from five 15 cm dishes per sample, where each experimental group contains three replicates without (as a negative control to identify non-specific 'background' proteins) and four replicates with UV cross-linked conditions. HL-1 cells were washed with cold PBS twice and cross-linked using 150 mJ/cm2 of 254 nm UV light. Cells were then lysed with lysis buffer, incubated 10 minutes on ice, homogenized by passing several times through a 21G needle and DNase digested with addition of DNase salt solution and Turbo DNase for 10 minutes at 37$^o$C (ThermoFisher, AM2238). Hybridization conditions were adjusted by the addition of an equal amount of hybridization buffer. Lysates were precleared with streptavidin-coated magnetic beads. Biotin labelled Gadlor1 and Gadlor2 probes were heated to 85$^o$C for three minutes and then incubated with the lysate for 2 hours at 67°C. Probe-RNA complexes were captured by pre-washed streptavidin coated magnetic beads and incubating at 37$^o$C for 30 minutes. Lysate was removed from beads by magnetic separation, and beads were washed four times in hybridization buffer at 67$^o$C. *Gadlor* RNA bound proteins were then released by Benzonase RNA digestion for two hours at 37$^o$C. The captured protein samples were identified by TMT labelling followed by liquid chromatography-mass spectroscopy (LC-MS/MS) by the EMBL proteomics core facility.

**RNA immunoprecipitation (RIP)**

We performed RIP with minor modifications to a previously described protocol to confirm the interaction of *Gadlor1* and *Gadlor2* lncRNAs with CaMKII and GLYR1. [48] HL-1 cardiomyocytes were used to overexpress *Gadlor* lncRNAs by adenovirus treatment, while Ad.βgal treated samples were used as control. Three 15 cm plates were combined for preparation of each sample. Briefly, cells were washed with ice-cold PBS twice and lysed with polysome lysis buffer (100 mM KCl, 5 mM MgCl2, 10 mM HEPES pH 7, 0.5% IGEPAL CA-630, 0.1 mM DTT, 1 x protease inhibitor cocktail, 1 x RNasIN). Cell lysates were passed through a 26G needle multiple times for homogenization. Protein G magnetic beads (Bio-Rad SureBeads, 161-4221) were washed twice with NT-2 buffer (50 mM Tris-HCl pH 7.4, 150 mM NaCl, 5 mM MgCl2, 0.05 % IGEPAL CA-630) and coupled with anti-CaMKII antibody (Santa Cruz, sc-5306), anti-GLYR1 antibody (Proteintech, 14833-1-AP) or anti-IgG (mouse, Cell Signaling 7076, as control) overnight at 4°C. Antibody coupled beads

were washed twice with NT-2 buffer and resuspended in NET-2 buffer (50 mM Tris-HCl pH 7.4, 150 mM NaCl, 5 mM MgCl2, 0.05 % IGEPAL CA-630, 20 mM EDTA pH 8, 1 mM DTT, 1 x RNaseIN). Cell lysates were added to beads and incubated at 4°C for 2 hours (10% lysate was removed as input and stored on ice prior to IP).

After supernatant was removed from beads, 1 ml of ice-cold NT-2 buffer was used to wash the beads five times in total. Then, beads were resuspended with Proteinase K buffer (1x NT-2 buffer and 1% SDS) and incubated at 55°C for 30 minutes with constant shaking while input sample conditions were adjusted accordingly and processed in parallel. Supernatant was transferred into fresh tubes and combined with NT-2 buffer and UltraPure phenol-chloroform (ThermoFisher, 15593031) for RNA purification. After centrifugation in heavy-lock tubes at 15.000 x g for 15 minutes, clear aqueous phase was purified with RNA Clean and concentrator kit (Zymo Research, R1017).

**DNA Isolation and Analysis of mtDNA/ nDNA**

To analyze the mitochondrial DNA (mtDNA) to nuclear DNA (nDNA) ratio of *Gadlor*-KO and WT mouse hearts after 2-weeks of TAC, genomic DNA was isolated from mouse heart tissue samples obtained after TAC (2w) with a DNA isolation kit according to manufacturers' instructions (PureLink Genomic DNA Mini kit, Invitrogen, K182001). The mtDNA/ nDNA ratios were quantified by quantitative PCR using ND1 and 16S rRNA primers listed in the **Supplemental Table 3**.

**Bulk RNA sequencing and Bioinformatics**

In order to perform RNA sequencing, RNA isolation was performed from isolated cells as described at indicated time-points (2 weeks after TAC or sham surgery). Quality control of RNA samples (Agilent 2100 Fragment Analyzer), and library preparation were performed by BGI, Hong Kong. Bulk RNA sequencing of different cardiac cells were performed as stranded and single-end by BGI. Initially, the trimming of adapter sequences from Fastq files was performed with the R package *FastqCleaner*. For aligning the reads to the reference genome (mm10) after trimming, the R package *bowtie2* alignment tool was used. Gene annotation was performed with *bioMaRt* R package. Library size of the samples were normalized to counts per million (cpm), and transformed into log2 values followed by calculation of differential gene expression with the *edgeR* package of R. Significant changes in gene expression between compared groups were filtered based on FDR < 0.05, and fold change (FC) > 1.5. Gene ontology analysis were performed with Metascape and DAVID online tools. Heatmaps that show the differentially regulated genes were generated by heatmap.2 function in *ggplot2* library in R.

RNAseq data-set is deposited in National Center for Biotechnology Information's Gene Expression Omnibus database with accession number GSE213612.

**Statistics**

Data analysis and statistical analysis were performed with GraphPad Prism software (Version 8). Data are shown as mean ± standard error of the mean (SEM). All the experiments were carried out in at least 3 biological replicates. The number of replicates for animal experiments and cell culture experiments are

indicated in the figure legends. The investigators were blinded for mouse genotype and treatment during surgeries, echocardiography, cardiac catheterization, organ weight determination and all histological and immunofluorescence quantifications.

Initially, all the datasets were analyzed for normality to allow the application of the proper statistical test. An unpaired 2-tailed Student t-test was used for comparing 2 groups only. Comparing multiple groups for one condition was performed with one-way ANOVA and Fisher's LSD post-hoc test. Comparing multiple groups for multiple conditions was achieved with two-way ANOVA and followed with Fisher's LSD post-hoc test when applicable. For non-parametric data sets, the Mann-Whitney and Kruksal-Willis tests were used to compare two groups and multiple groups, respectively. Values of $p<0.05$ were considered statistically significant.

**Acknowledgement**

The authors thank the Core Facilities Pre-Clinical Models, LIMA (Live Cell Imaging Mannheim) and FlowCore for comments and assistance, and the transgenic mouse service TGSM at HZI for generating the knockout mice. The authors gratefully acknowledge the data storage service SDS@hd supported by the Ministry of Science, Research and the Arts Baden-Württemberg (MWK).

**Author contributions**

**M.K** designed and performed the experiments, analyzed RNAseq data and wrote the first draft of the manuscript. **S.G.** designed and performed the experiments, and analyzed data. **N.F.**, **F.A.T.**, **R.W.**, **S.H., S.L.** and **G.M.D.** performed experiments. **D.W.** designed and supervised the generation of *Gadlor*-KO mice. **N.W.** maintained the mouse colonies and performed experiments. **S.U.** and **K.B.** provided experimental support for the study. **M.S, R.H, Ja.H.** and **D.F.** performed experiments. **A.M.G.** and **J.C.** provided experimental support and advice for the study. **No.F., J.B., G.D.** and **T. W.** provide crucial advice for the study and critically revised the paper. **J.H.** designed and conceptualized the study, supervised all the experiments and prepared the final draft of the manuscript. All authors read and approved the manuscript.

**Sources of Funding**

This study was supported by grants from SFB1366/1-A6 (J.H.) by the Deutsche Forschungsgemeinschaft.

**Disclosures**

The following patent has been granted: LncRNAs Gadlor1 and 2 for use in treating and preventing cardiac remodeling. US11208656 (granted 28.01.2021).

**References**


1. Tsao CW, Aday AW, Almarzooq ZI, Alonso A, Beaton AZ, Bittencourt MS, Boehme AK, Buxton AE, Carson AP, Commodore-Mensah Y, et al. Heart Disease and Stroke Statistics-2022 Update: A Report From the American Heart Association. *Circulation*. 2022;145:e153-e639. doi: 10.1161/CIR.0000000000001052
2. Frantz S, Hundertmark MJ, Schulz-Menger J, Bengel FM, Bauersachs J. Left ventricular remodelling post-myocardial infarction: pathophysiology, imaging, and novel therapies. *Eur Heart J*. 2022;43:2549-2561. doi: 10.1093/eurheartj/ehac223
3. Wu X, Reboll MR, Korf-Klingebiel M, Wollert KC. Angiogenesis after acute myocardial infarction. *Cardiovasc Res*. 2021;117:1257-1273. doi: 10.1093/cvr/cvaa287
4. Frey N, Katus HA, Olson EN, Hill JA. Hypertrophy of the heart: a new therapeutic target? *Circulation*. 2004;109:1580-1589. doi: 10.1161/01.CIR.0000120390.68287.BB
5. Bar C, Chatterjee S, Falcao Pires I, Rodrigues P, Sluijter JPG, Boon RA, Nevado RM, Andres V, Sansonetti M, de Windt L, et al. Non-coding RNAs: update on mechanisms and therapeutic targets from the ESC Working Groups of Myocardial Function and Cellular Biology of the Heart. *Cardiovasc Res*. 2020;116:1805-1819. doi: 10.1093/cvr/cvaa195
6. Hill JA, Olson EN. Cardiac plasticity. *N Engl J Med*. 2008;358:1370-1380. doi: 10.1056/NEJMra072139
7. Heineke J, Molkentin JD. Regulation of cardiac hypertrophy by intracellular signalling pathways. *Nat Rev Mol Cell Biol*. 2006;7:589-600. doi: 10.1038/nrm1983
8. Huang CK, Kafert-Kasting S, Thum T. Preclinical and Clinical Development of Noncoding RNA Therapeutics for Cardiovascular Disease. *Circ Res*. 2020;126:663-678. doi: 10.1161/CIRCRESAHA.119.315856
9. Lu D, Thum T. RNA-based diagnostic and therapeutic strategies for cardiovascular disease. *Nat Rev Cardiol*. 2019;16:661-674. doi: 10.1038/s41569-019-0218-x
10. Wilusz JE, Sunwoo H, Spector DL. Long noncoding RNAs: functional surprises from the RNA world. *Genes Dev*. 2009;23:1494-1504. doi: 10.1101/gad.1800909
11. Li H, Trager LE, Liu X, Hastings MH, Xiao C, Guerra J, To S, Li G, Yeri A, Rodosthenous R, et al. lncExACT1 and DCHS2 Regulate Physiological and Pathological Cardiac Growth. *Circulation*. 2022;145:1218-1233. doi: 10.1161/CIRCULATIONAHA.121.056850
12. Zhao Y, Riching AS, Knight WE, Chi C, Broadwell LJ, Du Y, Abdel-Hafiz M, Ambardekar AV, Irwin DC, Proenza C, et al. Cardiomyocyte-Specific Long Noncoding RNA Regulates Alternative Splicing of the Triadin Gene in the Heart. *Circulation*. 2022;146:699-714. doi: 10.1161/CIRCULATIONAHA.121.058017
13. Viereck J, Kumarswamy R, Foinquinos A, Xiao K, Avramopoulos P, Kunz M, Dittrich M, Maetzig T, Zimmer K, Remke J, et al. Long noncoding RNA Chast promotes cardiac remodeling. *Sci Transl Med*. 2016;8:326ra322. doi: 10.1126/scitranslmed.aaf1475
14. Han P, Li W, Lin CH, Yang J, Shang C, Nuernberg ST, Jin KK, Xu W, Lin CY, Lin CJ, et al. A long noncoding RNA protects the heart from pathological hypertrophy. *Nature*. 2014;514:102-106. doi: 10.1038/nature13596
15. Cheng Y, Wang X, Yang J, Duan X, Yao Y, Shi X, Chen Z, Fan Z, Liu X, Qin S, et al. A translational study of urine miRNAs in acute myocardial infarction. *J Mol Cell Cardiol*. 2012;53:668-676. doi: 10.1016/j.yjmcc.2012.08.010
16. Kuwabara Y, Ono K, Horie T, Nishi H, Nagao K, Kinoshita M, Watanabe S, Baba O, Kojima Y, Shizuta S, et al. Increased microRNA-1 and microRNA-133a levels in serum of patients with cardiovascular disease indicate myocardial damage. *Circ Cardiovasc Genet*. 2011;4:446-454. doi: 10.1161/CIRCGENETICS.110.958975

17. Schulte C, Barwari T, Joshi A, Zeller T, Mayr M. Noncoding RNAs versus Protein Biomarkers in Cardiovascular Disease. *Trends Mol Med*. 2020;26:583-596. doi: 10.1016/j.molmed.2020.02.001
18. Sluijter JP, Verhage V, Deddens JC, van den Akker F, Doevendans PA. Microvesicles and exosomes for intracardiac communication. *Cardiovasc Res*. 2014;102:302-311. doi: 10.1093/cvr/cvu022
19. Pinto AR, Ilinykh A, Ivey MJ, Kuwabara JT, D'Antoni ML, Debuque R, Chandran A, Wang L, Arora K, Rosenthal NA, et al. Revisiting Cardiac Cellular Composition. *Circ Res*. 2016;118:400-409. doi: 10.1161/CIRCRESAHA.115.307778
20. Uchida S, Dimmeler S. Long noncoding RNAs in cardiovascular diseases. *Circ Res*. 2015;116:737-750. doi: 10.1161/CIRCRESAHA.116.302521
21. Kenneweg F, Bang C, Xiao K, Boulanger CM, Loyer X, Mazlan S, Schroen B, Hermans-Beijnsberger S, Foinquinos A, Hirt MN, et al. Long Noncoding RNA-Enriched Vesicles Secreted by Hypoxic Cardiomyocytes Drive Cardiac Fibrosis. *Mol Ther Nucleic Acids*. 2019;18:363-374. doi: 10.1016/j.omtn.2019.09.003
22. Piccoli MT, Gupta SK, Viereck J, Foinquinos A, Samolovac S, Kramer FL, Garg A, Remke J, Zimmer K, Batkai S, et al. Inhibition of the Cardiac Fibroblast-Enriched lncRNA Meg3 Prevents Cardiac Fibrosis and Diastolic Dysfunction. *Circ Res*. 2017;121:575-583. doi: 10.1161/CIRCRESAHA.117.310624
23. Hosen MR, Li Q, Liu Y, Zietzer A, Maus K, Goody P, Uchida S, Latz E, Werner N, Nickenig G, et al. CAD increases the long noncoding RNA PUNISHER in small extracellular vesicles and regulates endothelial cell function via vesicular shuttling. *Mol Ther Nucleic Acids*. 2021;25:388-405. doi: 10.1016/j.omtn.2021.05.023
24. Bang C, Batkai S, Dangwal S, Gupta SK, Foinquinos A, Holzmann A, Just A, Remke J, Zimmer K, Zeug A, et al. Cardiac fibroblast-derived microRNA passenger strand-enriched exosomes mediate cardiomyocyte hypertrophy. *J Clin Invest*. 2014;124:2136-2146. doi: 10.1172/JCI70577
25. Hosen MR, Goody PR, Zietzer A, Xiang X, Niepmann ST, Sedaghat A, Tiyerili V, Chennupati R, Moore JBt, Boon RA, et al. Circulating MicroRNA-122-5p Is Associated With a Lack of Improvement in Left Ventricular Function After Transcatheter Aortic Valve Replacement and Regulates Viability of Cardiomyocytes Through Extracellular Vesicles. *Circulation*. 2022:101161CIRCULATIONAHA122060258. doi: 10.1161/CIRCULATIONAHA.122.060258
26. Huang G, Garikipati VNS, Zhou Y, Benedict C, Houser SR, Koch WJ, Kishore R. Identification and Comparison of Hyperglycemia-Induced Extracellular Vesicle Transcriptome in Different Mouse Stem Cells. *Cells*. 2020;9. doi: 10.3390/cells9092098
27. Froese N, Cordero J, Abouissa A, Trogisch FA, Grein S, Szaroszyk M, Wang Y, Gigina A, Korf-Klingebiel M, Bosnjak B, et al. Analysis of myocardial cellular gene expression during pressure overload reveals matrix based functional intercellular communication. *iScience*. 2022;25:103965. doi: 10.1016/j.isci.2022.103965
28. Das S, Shah R, Dimmeler S, Freedman JE, Holley C, Lee JM, Moore K, Musunuru K, Wang DZ, Xiao J, et al. Noncoding RNAs in Cardiovascular Disease: Current Knowledge, Tools and Technologies for Investigation, and Future Directions: A Scientific Statement From the American Heart Association. *Circ Genom Precis Med*. 2020;13:e000062. doi: 10.1161/HCG.0000000000000062
29. Heineke J, Auger-Messier M, Xu J, Oka T, Sargent MA, York A, Klevitsky R, Vaikunth S, Duncan SA, Aronow BJ, et al. Cardiomyocyte GATA4 functions as a stress-responsive regulator of angiogenesis in the murine heart. *J Clin Invest*. 2007;117:3198-3210. doi: 10.1172/JCI32573
30. Dittrich GM, Froese N, Wang X, Kroeger H, Wang H, Szaroszyk M, Malek-Mohammadi M, Cordero J, Keles M, Korf-Klingebiel M, et al. Fibroblast GATA-4 and GATA-6 promote myocardial adaptation to pressure overload by enhancing cardiac angiogenesis. *Basic Res Cardiol*. 2021;116:26. doi: 10.1007/s00395-021-00862-y

31. Sano M, Minamino T, Toko H, Miyauchi H, Orimo M, Qin Y, Akazawa H, Tateno K, Kayama Y, Harada M, et al. p53-induced inhibition of Hif-1 causes cardiac dysfunction during pressure overload. *Nature*. 2007;446:444-448. doi: 10.1038/nature05602
32. Vidal R, Wagner JUG, Braeuning C, Fischer C, Patrick R, Tombor L, Muhly-Reinholz M, John D, Kliem M, Conrad T, et al. Transcriptional heterogeneity of fibroblasts is a hallmark of the aging heart. *JCI Insight*. 2019;4. doi: 10.1172/jci.insight.131092
33. Kim KM, Abdelmohsen K, Mustapic M, Kapogiannis D, Gorospe M. RNA in extracellular vesicles. *Wiley Interdiscip Rev RNA*. 2017;8. doi: 10.1002/wrna.1413
34. Pironti G, Strachan RT, Abraham D, Mon-Wei Yu S, Chen M, Chen W, Hanada K, Mao L, Watson LJ, Rockman HA. Circulating Exosomes Induced by Cardiac Pressure Overload Contain Functional Angiotensin II Type 1 Receptors. *Circulation*. 2015;131:2120-2130. doi: 10.1161/CIRCULATIONAHA.115.015687
35. Fei J, Ishii H, Hoeksema MA, Meitinger F, Kassavetis GA, Glass CK, Ren B, Kadonaga JT. NDF, a nucleosome-destabilizing factor that facilitates transcription through nucleosomes. *Genes Dev*. 2018;32:682-694. doi: 10.1101/gad.313973.118
36. Mattiazzi A, Bassani RA, Escobar AL, Palomeque J, Valverde CA, Vila Petroff M, Bers DM. Chasing cardiac physiology and pathology down the CaMKII cascade. *Am J Physiol Heart Circ Physiol*. 2015;308:H1177-1191. doi: 10.1152/ajpheart.00007.2015
37. Kirchhefer U, Schmitz W, Scholz H, Neumann J. Activity of cAMP-dependent protein kinase and Ca2+/calmodulin-dependent protein kinase in failing and nonfailing human hearts. *Cardiovasc Res*. 1999;42:254-261. doi: 10.1016/s0008-6363(98)00296-x
38. Backs J, Backs T, Neef S, Kreusser MM, Lehmann LH, Patrick DM, Grueter CE, Qi X, Richardson JA, Hill JA, et al. The delta isoform of CaM kinase II is required for pathological cardiac hypertrophy and remodeling after pressure overload. *Proc Natl Acad Sci U S A*. 2009;106:2342-2347. doi: 10.1073/pnas.0813013106
39. Li C, Cai X, Sun H, Bai T, Zheng X, Zhou XW, Chen X, Gill DL, Li J, Tang XD. The deltaA isoform of calmodulin kinase II mediates pathological cardiac hypertrophy by interfering with the HDAC4-MEF2 signaling pathway. *Biochem Biophys Res Commun*. 2011;409:125-130. doi: 10.1016/j.bbrc.2011.04.128
40. Beckendorf J, van den Hoogenhof MMG, Backs J. Physiological and unappreciated roles of CaMKII in the heart. *Basic Res Cardiol*. 2018;113:29. doi: 10.1007/s00395-018-0688-8
41. Mattiazzi A, Kranias EG. The role of CaMKII regulation of phospholamban activity in heart disease. *Front Pharmacol*. 2014;5:5. doi: 10.3389/fphar.2014.00005
42. Kemi OJ, Ellingsen O, Ceci M, Grimaldi S, Smith GL, Condorelli G, Wisloff U. Aerobic interval training enhances cardiomyocyte contractility and Ca2+ cycling by phosphorylation of CaMKII and Thr-17 of phospholamban. *J Mol Cell Cardiol*. 2007;43:354-361. doi: 10.1016/j.yjmcc.2007.06.013
43. Louch WE, Sheehan KA, Wolska BM. Methods in cardiomyocyte isolation, culture, and gene transfer. *J Mol Cell Cardiol*. 2011;51:288-298. doi: 10.1016/j.yjmcc.2011.06.012
44. Prendergast EN, de Souza Fonseca MA, Dezem FS, Lester J, Karlan BY, Noushmehr H, Lin X, Lawrenson K. Optimizing exosomal RNA isolation for RNA-Seq analyses of archival sera specimens. *PLoS One*. 2018;13:e0196913. doi: 10.1371/journal.pone.0196913
45. Grund A, Szaroszyk M, Korf-Klingebiel M, Malek Mohammadi M, Trogisch FA, Schrameck U, Gigina A, Tiedje C, Gaestel M, Kraft T, et al. TIP30 counteracts cardiac hypertrophy and failure by inhibiting translational elongation. *EMBO Mol Med*. 2019;11:e10018. doi: 10.15252/emmm.201810018
46. Tetzlaff F, Fischer A. Human Endothelial Cell Spheroid-based Sprouting Angiogenesis Assay in Collagen. *Bio Protoc*. 2018;8:e2995. doi: 10.21769/BioProtoc.2995

47. McHugh CA, Guttman M. RAP-MS: A Method to Identify Proteins that Interact Directly with a Specific RNA Molecule in Cells. *Methods Mol Biol*. 2018;1649:473-488. doi: 10.1007/978-1-4939-7213-5_31
48. Gagliardi M, Matarazzo MR. RIP: RNA Immunoprecipitation. *Methods Mol Biol*. 2016;1480:73-86. doi: 10.1007/978-1-4939-6380-5_7

**Supplemental Tables**

**Table 1:** List of primers used for genotyping of *Gadlor*-KO mouse line

| | **Primer 1 (Forward)** | **Primer 2 (Reverse)** |
|---|---|---|
| ***Gadlor*-WT** | CTTGAGCCGTCTCTCCAAAG | GGGTGGCATGCAAGATGATTGAGA |
| ***Gadlor*-KO** | CTTGAGCCGTCTCTCCAAAG | TGTGGAGTGGACACATAGAGG |

**Table 2:** List of antibodies used in cell isolation methodologies and immunofluorescence (IF) staining.

| **Target** | **Company, Catalogue No** | **Application** |
|---|---|---|
| **Anti-mouse CD146 (LSEC) MicroBeads** | Miltenyi-Biotec, 130-092-007 | Cell isolation |
| **Feeder Removal MicroBeads, Mouse** | Miltenyi-Biotec, 130-095-531 | Cell isolation |
| **Isolectin B4 (IB4)** | Vector Lab, FL-1201 | 1:50 (IF) |
| **Purified Rat Anti-mouse CD102** | BD Pharmingen, 553326 | Cell isolation |
| **Purified Rat Anti-mouse CD31** | BD Pharmingen, 553370 | Cell isolation |
| **Rabbit Polyclonal anti-ki67** | Abcam, ab15580 | 1:100 (IF) |
| **VECTASHIELD HardSet Antifade Mounting Medium With DAPI** | Vector Lab, H-1500 | |
| **Wheat Germ Agglutinin (WGA)** | Invitrogen, W21405 | 1:100 (IF) |

**Table 3:** List of primers used for qPCR and qRT-PCR.

| | **Primer 1 (Forward)** | **Primer 2 (Reverse)** |
|---|---|---|
| ***Gadlor1*** | AGGTGAGCTCTGGTTGTGTT | CTGCTGCCTGTGAAAGATGG |
| ***Gadlor2*** | TGAGACTCCACTTGCCACAT | TGTGGTTTCAGGCATGTTTCT |
| ***GADLOR1*** | AATTTCAGCCACAAGCATCC | TGCTTGGGGAAGAGGAAGTA |
| ***GADLOR2*** | TGGGATCTAAGCACTGACACC | GAGACAGACATTCGTTTGGTCA |
| **18S** | GTAACCCGTTGAACCCCATT | CCATCCAATCGGTAGTAGCG |
| **U6** | CTCGCTTCGGCAGCACA | AACGCTTCACGAATTTGCGT |
| ***Gapdh*** | CGTCCCGTAGACAAAATGGT | GAATTTGCCGTGAGTGGAGT |
| ***Acat1*** | GCAGGGAAGTTTGCCAGTGAGA | GAACACGGTCTTGAGCTTTGGC |
| ***Actn2*** | CACCTGGAGTTTGCCAAGAGAG | GCCTTGAACTGCTCATGTGCAG |
| ***Adam8*** | TGCCAACGTGACACTGGAGAAC | GCAGACACCTTAGCCAGTCCAA |
| ***Angpt2*** | AACTCGCTCCTTCAGAAGCAGC | TTCCGCACAGTCTCTGAAGGTG |
| ***Angptl4*** | CTGGACAGTGATTCAGAGACGC | GATGCTGTGCATCTTTTCCAGGC |
| ***Aurkb*** | CTTCTACGACCAGCAGAGGATC | GGCATCTGACAGTTCCTCCATG |
| ***Cacna1c*** | CGTTCTCATCCTGCTCAACACC | GAGCTTCAGGATCATCTCCACTG |
| ***Camk2d*** | GTGACACCTGAAGCCAAAGACC | CCTGTGCATCATGGAGGCAACA |
| ***Cdk1*** | CATGGACCTCAAGAAGTACCTGG | CAAGTCTCTGTGAAGAACTCGCC |
| ***Col15a1*** | ACACCCACAGTGACTCCCAAGA | TCCTCATTGCCCACGATGTCTC |
| ***Col1a1*** | CCGCTGGTCAAGATGGTC | CCTCGCTCTCCAGCCTTT |
| ***Col3a1*** | ATAAGCCCTGATGGTTCTCG | ATGCATGTTTCCCCAGTTTC |
| ***Col4a1*** | ATGGCTTGCCTGGAGAGATAGG | TGGTTGCCCTTTGAGTCCTGGA |
| ***Col6a1*** | GACACCTCTCAGTGTGCTCTGT | GCGATAAGCCTTGGCAGGAAATG |
| ***Comp*** | GTGCCCAACTTTGACCAGAGTG | ACAGGCATCACCCACAAAGTCG |

| | | |
|---|---|---|
| ***Cox5a*** | GTCACACGAGACAGATGAGGAG | CCGTCTACATGCTCGCAATGCA |
| ***Cxcl2*** | CATCCAGAGCTTGAGTGTGACG | GGCTTCAGGGTCAAGGCAAACT |
| ***Dll1*** | GCTGGAAGTAGATGAGTGTGCTC | CACAGACCTTGCCATAGAAGCC |
| ***Efna1*** | GCTGAAGGTGACTGTCAATGGC | CGGCACTGTAACCAATGCTGTG |
| ***Fgfr2*** | GTCTCCGAGTATGAGTTGCCAG | CCACTGCTTCAGCCATGACTAC |
| ***Fh1*** | GAACTCACACGCAGGATGCTGT | GGCGGCTTTTATTCTCACCATCG |
| ***Fn1*** | TGTGACAACTGCCGTAGACC | TGGGGTGTGGATTGACCTTG |
| ***Gata4*** | GCCTCTATCACAAGATGAACGGC | TACAGGCTCACCCTCGGCATTA |
| ***Icam5*** | ACCGATGCACAGCAGTCAATGG | ATGTTCTGGGCAGCCTACACTG |
| ***Igf1*** | GTGGATGCTCTTCAGTTCGTGTG | TCCAGTCTCCTCAGATCACAGC |
| ***Il6*** | CGGCCTTCCCTACTTCACAA | TCCAGTTTGGTAGCATCCATCA |
| ***Klf15*** | ACACCAAGAGCAGCCACCTCAA | GCCTTGACAACTCATCTGAGCG |
| ***Lsamp*** | GGAGTCGAAGAGCAACGAAG | AATCTCAAGGCCATTTGCAC |
| ***Mfn2*** | GTGGAATACGCCAGTGAGAAGC | CAACTTGCTGGCACAGATGAGC |
| ***Myh6*** | GAGTGGGAGTTTATCGACTTCG | CCTTGACATTGCGAGGCTTC |
| ***Myh7*** | ACTGTCAACACTAAGAGGGTCA | TTGGATGATTTGATCTTCCAGGG |
| ***Nppa*** | TTCCTCGTCTTGGCCTTTTG | CCTCATCTTCTACCGGCATC |
| ***Nppb*** | GTCCAGCAGAGACCTCAAAA | AGGCAGAGTCAGAAACTGGA |
| ***Rcan1.4*** | CTTGTGTGGCAAACGATGATG | TGGTGTCCTTGTCATATGTTCTG |
| ***Sirt1*** | GGAGCAGATTAGTAAGCGGCTTG | GTTACTGCCACAGGAACTAGAGG |
| ***Sucla2*** | GGTGTCTCTGTTCCCAAAGGCT | TTTCCTCTGCCGCCAGCCAAAA |
| ***Tlr9*** | GCTGTCAATGGCTCTCAGTTCC | CCTGCAACTGTGGTAGCTCACT |
| ***ND1*** | CTAGCAGAAACAAACCGGGC | CCGGCTGCGTATTCTACGTT |
| ***16S*** | CCGCAAGGGAAAGATGAAAGAC | TCGTTTGGTTTCGGGGTTTC |

**Table 4:** List of *Gadlor1* and *Gadlor2* probes used for RNA antisense purification (RAP).

| | **Probe Sequence** |
|---|---|
| ***Gadlor1* – Probe 1** | [Btn]AGGATTGTTAAATATGACTATGCTTGGTATAGTCACAAAACATGGGAGTAC |
| ***Gadlor1* – Probe 2** | [Btn]TATCATAATCTTTCTGTAGGCCATTACTTGTTTCATATTTTAAAGGGACAG TCCACTCTAGGAATGTCAAGTGTCTGATCTCTGAAAACA |
| ***Gadlor1* – Probe 3** | [Btn]TTTTCTGAATAGTTGAAAATTCTAACTAAACACAGGAAGAACAGAGNCAC AAGAATAAAGAAATTTAGATATATCCTAAATGTTTCCAGG |
| ***Gadlor1* – Probe 4** | [Btn]ATAAAAGAAGGCGAGGGGTGGCATGCAAGATGATTGAGAAAGCCCAGT AGCCATTTTTGGGGTGGGGCAAAGGGAGTGGTCTGGGTAGGG |
| ***Gadlor2* – Probe 1** | [Btn]GCTGCTATTTTATTATCTCTTTGGTTCTGTTTTTCATTTGTATTAAAAATG |
| ***Gadlor2* – Probe 2** | [Btn]GTGATGGTGAAGATGAAATTGAGATGAATCATTTGAAGAACGATGTGCGTT TTAGAAGAATCACTTTGTC |

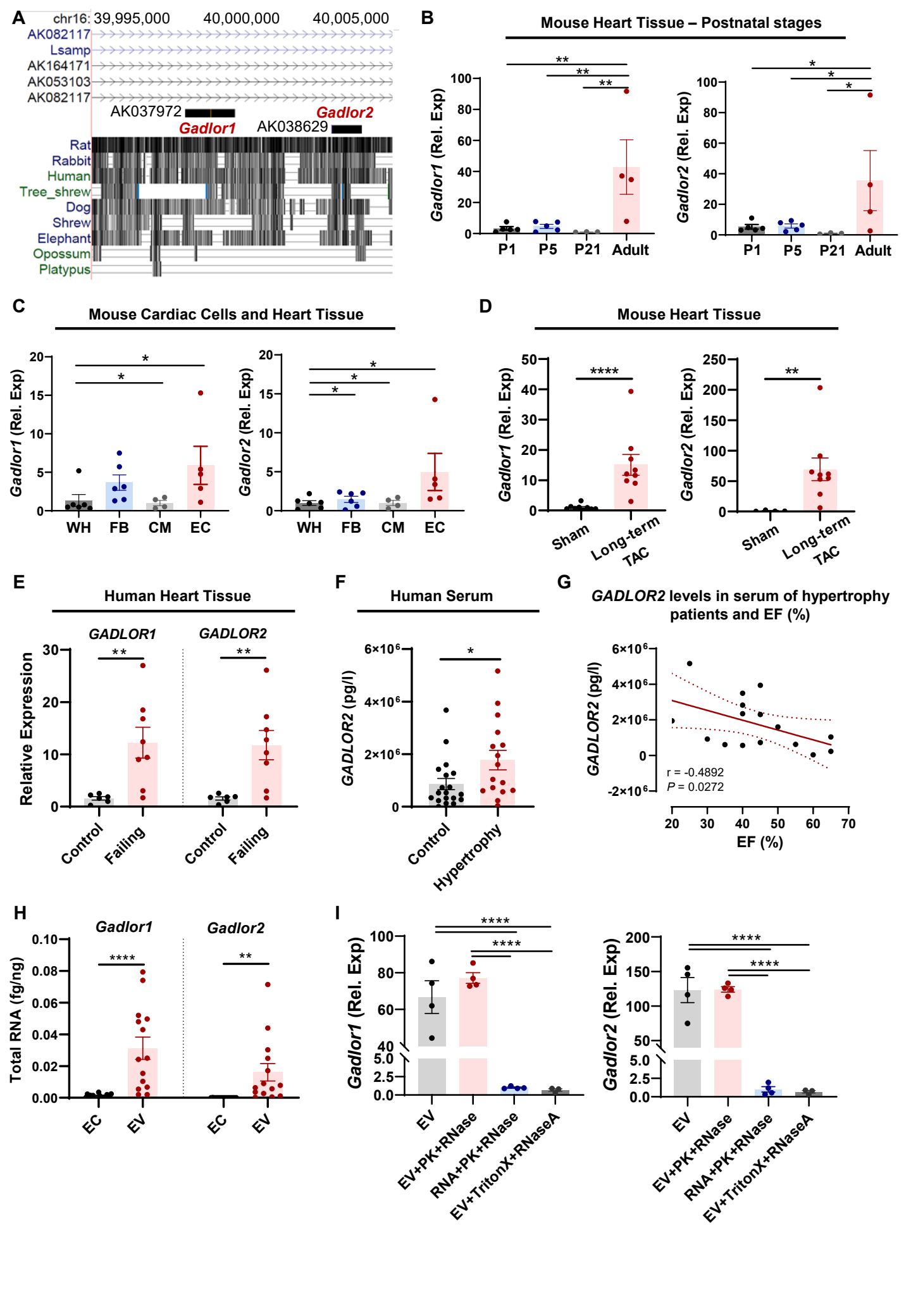
A
chr16: 39,995,000
40,000,000
40,005,000
AK082117
Lsamp
AK164171
AK053103
AK082117
AK037972
Gadlor1
Gadlor2
AK038629
Rat
Rabbit
Human
Tree_shrew
Dog
Shrew
Elephant
Opossum
Platypus
B
Mouse Heart Tissue – Postnatal stages
Gadlor1 (Rel. Exp)
Gadlor2 (Rel. Exp)
P1
P5
P21
Adult
C
Mouse Cardiac Cells and Heart Tissue
WH
FB
CM
EC
D
Mouse Heart Tissue
Sham
Long-term TAC
E
Human Heart Tissue
GADLOR1
GADLOR2
Relative Expression
Control
Failing
F
Human Serum
GADLOR2 (pg/l)
Hypertrophy
G
GADLOR2 levels in serum of hypertrophy patients and EF (%)
r = -0.4892
P = 0.0272
EF (%)
H
Total RNA (fg/ng)
EC
EV
I
EV
EV+PK+RNase
RNA+PK+RNase
EV+TritonX+RNaseA

**Figure 1: *Gadlor* lncRNAs *are* mainly expressed in cardiac endothelial cells (ECs) and their expression is highly increased in mice after pressure-overload and in human failing hearts.**

**A.** UCSC Genome Browser visualization of AK037972 *(Gadlor1)* and AK038629 *(Gadlor2)* on mouse chromosome 16 and evolutionary conservation between different species. **B.** *Gadlor1* and *Gadlor2* expression levels in mouse cardiac tissue from different post-natal developmental stages (P1 – n=5, P5 – n= 5, P21 – n=3 and adult (9-weeks old) – n=4), and in **C.** different cardiac cell-types (EC: endothelial cells – n=5, FB: fibroblast – n=6, CM: cardiomyocytes – n=4) and heart tissue (WH: whole heart – n=6). **D.** *Gadlor* lncRNA levels in mouse cardiac tissue after long-term (12 weeks, n=9) TAC (transverse aortic constriction) compared to sham. **E.** *GADLOR1* and *2* expression in control (healthy, n=6) and human failing heart tissue (n=8) samples that were obtained from aortic stenosis patients. **F.** Detection of *GADLOR2* levels (pg/l: picogram/liter) in human serum of healthy volunteers (n=19) and patients with aortic stenosis (n=16). **G.** Correlation analysis of *GADLOR2* levels (pg/l) with ejection fraction (%) of hypertrophy patients (n=16), (Pearson correlation, Pearson r= -4892 and p-value = 0.0272). **H.** Absolute quantification of total RNA amount of *Gadlor1* and *Gadlor2* in ECs and EC-derived EVs (fg/ng: femtogram/ nanogram). **I.** Detection of *Gadlor* lncRNAs in EC-derived EVs with proteinase K (PK), RNase or Triton-X as indicated.
Data are shown as mean±SEM. Data normality was evaluated with the Shapiro-Wilk test. *P*-values were calculated with Student's t-test for parametric (or Mann-Whitney for non-parametric) for comparing two groups, and one-way ANOVA was applied for comparing multiple groups followed with Fisher's LSD post-hoc test. *p-value<0.05, **p-value<0.01, ***p-value<0.001, ****p-value<0.0001.

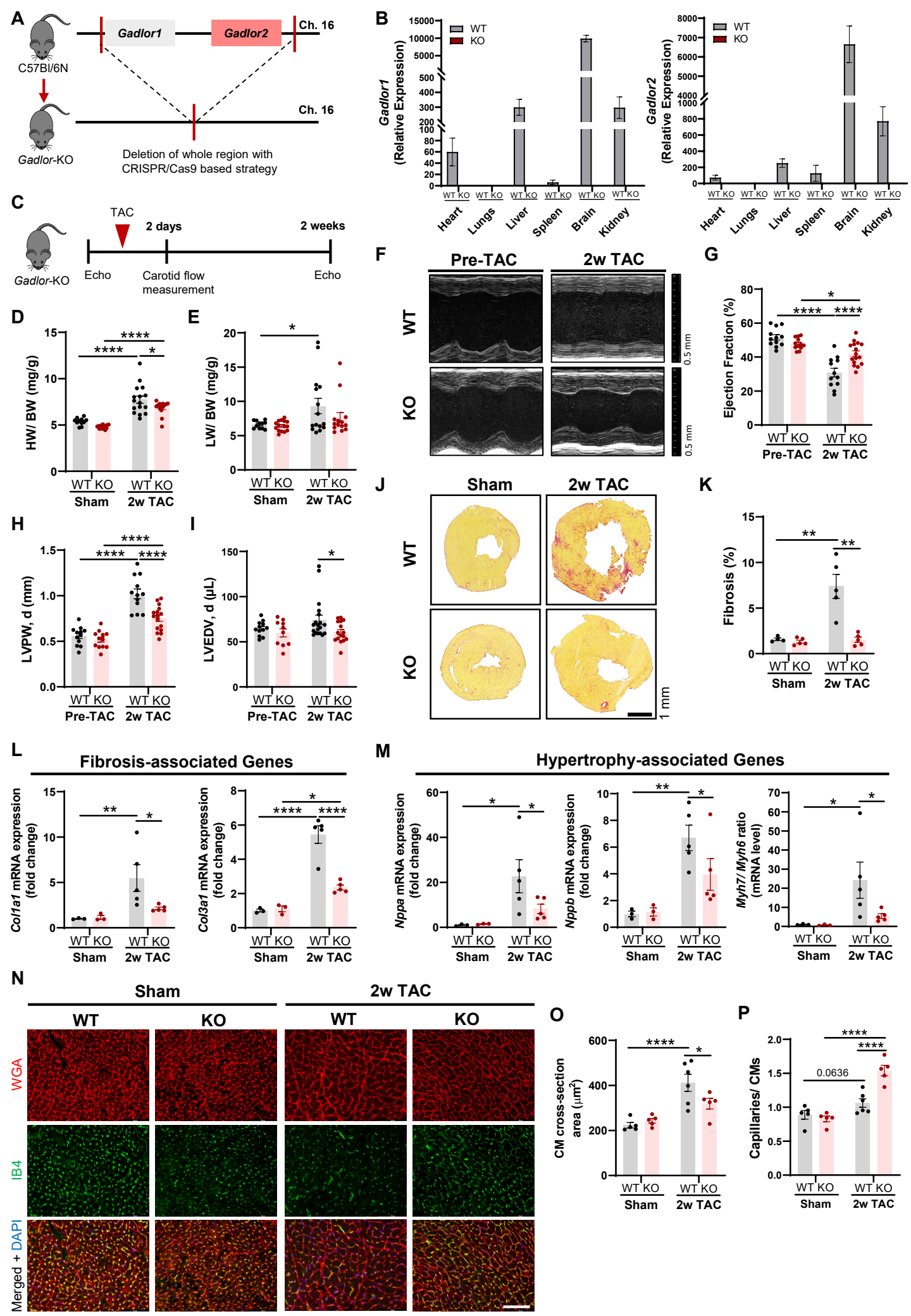
A
C57Bl/6N
Gadlor1
Gadlor2
Ch. 16
Ch. 16
Gadlor-KO
Deletion of whole region with CRISPR/Cas9 based strategy
B
WT
KO
Gadlor1 (Relative Expression)
Gadlor2 (Relative Expression)
Heart
Lungs
Liver
Spleen
Brain
Kidney
C
TAC
2 days
2 weeks
Gadlor-KO
Echo
Carotid flow measurement
Echo
D
HW/ BW (mg/g)
E
LW/ BW (mg/g)
Sham
2w TAC
F
Pre-TAC
2w TAC
WT
KO
0.5 mm
G
Ejection Fraction (%)
Pre-TAC
2w TAC
H
LVPW, d (mm)
I
LVEDV, d (µL)
J
Sham
2w TAC
1 mm
K
Fibrosis (%)
L
Fibrosis-associated Genes
Col1a1 mRNA expression (fold change)
Col3a1 mRNA expression (fold change)
M
Hypertrophy-associated Genes
Nppa mRNA expression (fold change)
Nppb mRNA expression (fold change)
Myh7/ Myh6 ratio (mRNA level)
N
Sham
2w TAC
WT
KO
WGA
IB4
Merged + DAPI
O
CM cross-section area (µm²)
P
Capillaries/ CMs
0.0636

**Figure 2: Deletion of *Gadlor* lncRNAs reduces cardiac hypertrophy and fibrosis after cardiac pressure overload.**

**A.** Scheme of *Gadlor*-KO mouse line generation by systemic deletion of the region on chromosome 16 containing both *Gadlor1* and *Gadlor2* by a CRISPR/Cas9 approach. **B.** Validation of *Gadlor*-KO mouse line by assessing the relative expression of *Gadlor*s in indicated organs in adult WT and *Gadlor*-KO mice (n≥8). The difference in *Gadlor1/2* expression levels between WT and *Gadlor*-KO animals were significant for all organs in which *Gadlor1* and *Gadlor2* were detected. (Heart: *p-value<0.05, Liver and Kidney: ***p-value<0.001, Brain: ****p-value<0.0001). **C.** Experimental design of TAC operation for *Gadlor*-KO and WT littermates. **D.** Heart weight (miligrams) to body weight (grams) ratio (HW/BW) and **E.** lung weight (miligrams) to body weight (grams) ratio of *Gadlor*-KO and WT littermates in sham and after 2 weeks TAC (n≥11). **F.** Representative echocardiography images of *Gadlor*-KO and WT mice before (pre-TAC) and after 2 weeks of TAC (2w TAC) shown in parasternal long axis mode, and analysis of **G.** left ventricle (LV) ejection fraction (EF%), **H.** LV posterior wall thickness in diastole (mm) and **I.** LV end diastolic volume (ul), (n≥12). **J.** Representative Sirius-red fibrosis staining in cardiac tissue sections of sham and 2w TAC animals (scale-bar: 1 mm) and **K.** quantification of fibrotic area (n≥4). **L.** Relative expression of fibrosis marker genes *Col1a1* and *Col3a1* and **M.** hypertrophy marker genes *Nppa, Nppb* and *Mhy7/6* ratio in mRNA levels in heart tissue samples of sham (n=3) and 2w TAC (n=5). **N.** Representative immunofluorescence images of cardiac tissue samples stained with WGA (wheat-germ agglutinin coupled with Alexa Fluor 555) and IB4 (Isolectin B4 coupled with Alexa Fluor 488) in sham and 2 week TAC samples from *Gadlor*-KO and WT littermates, scale-bar: 100 µm. Quantification of **O.** cardiomyocyte cross-sectional area and **P.** myocardial capillary density per cardiomyocyte ratio.
Data are shown as mean±SEM. Data normality was evaluated with Shapiro-Wilk test and p-values were calculated with Student's t-test for comparing two groups and two-way ANOVA for grouped analysis followed with Fisher's LSD post-hoc test. *p-value<0.05, **p-value<0.01, ***p-value<0.001, ****p-value<0.0001.

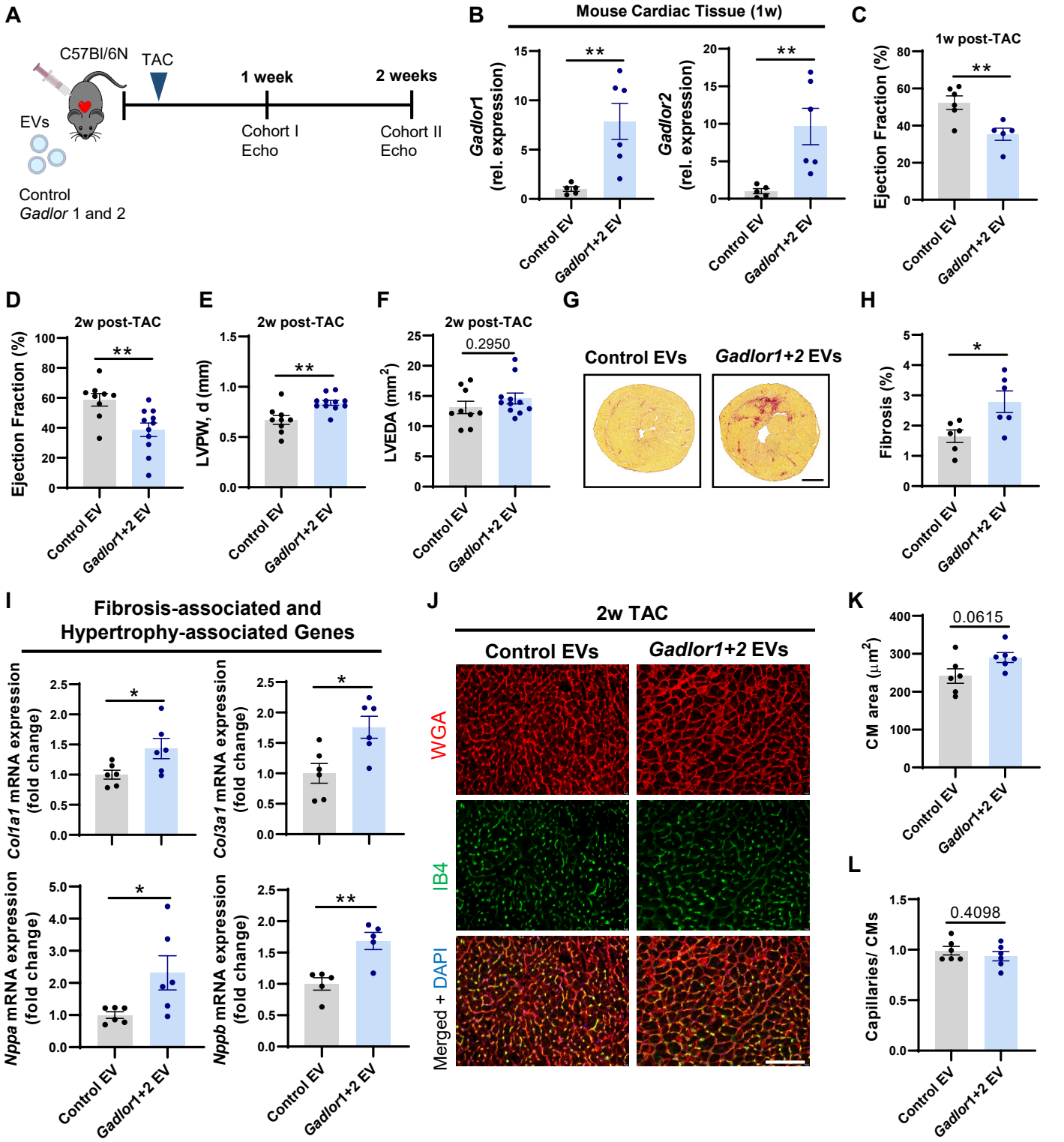


**Figure 3: Overexpression of *Gadlor1* and *Gadlor2* via extracellular vesicles triggers cardiac dysfunction and development of fibrosis after TAC.**

**A.** Scheme of the experimental design depicting the injection of *Gadlor1 and Gadlor2* containing extracellular vesicles for overexpression followed by TAC operation. **B.** Relative expression of *Gadlor1 and Gadlor2* in cardiac tissue samples after 1 week TAC (indicated as cohort I) to validate the overexpression after injection of control (Ad.βgal treated samples, n=5) and *Gadlor*-containing (Ad.Gadlor1 and Ad.Gadlor2 treated samples, n=6) EVs. Echocardiographic analysis of **C.** left ventricle (LV) ejection fraction (EF%) after 1 week TAC, and **D.** LV-EF%, **E.** LV posterior wall thickness in diastole (mm), **F.** LV-end diastolic area ($mm^2$) after 2 weeks TAC in mice injected with control EVs and *Gadlor*1 and *Gadlor2* EVs. **G.** Representative images of Sirius-red staining (scale bar: 1 mm) and **H.** quantification of fibrotic area after 2 weeks TAC in mice injected with control EVs and *Gadlor*1 and *2* EVs. **I.** Relative expression of fibrosis marker genes *Col1a1* and *Col3a1* and hypertrophy marker genes *Nppa* and *Nppb* in heart tissue samples of control-EV (n=6) and *Gadlor*-EVs (n=6) treated mice. **J.** Representative immunofluorescence images of cardiac tissue samples stained with WGA (wheat-germ agglutinin coupled with Alexa Fluor 555) and IB4 (Isolectin B4 coupled with Alexa Fluor 488) in samples from control EV and *Gadlor*-EV treated animals (scale-bar: 100 μm). Quantification of **K.** cardiomyocyte cross-sectional area and **L.** myocardial capillarization after EV treatment followed by 2 weeks of TAC. Data are shown as mean±SEM. Data normality was evaluated with Shapiro-Wilk test and p-values were calculated with Student's t-test. *p-value<0.05, **p-value<0.01, ***p-value<0.001, ****p-value<0.0001.

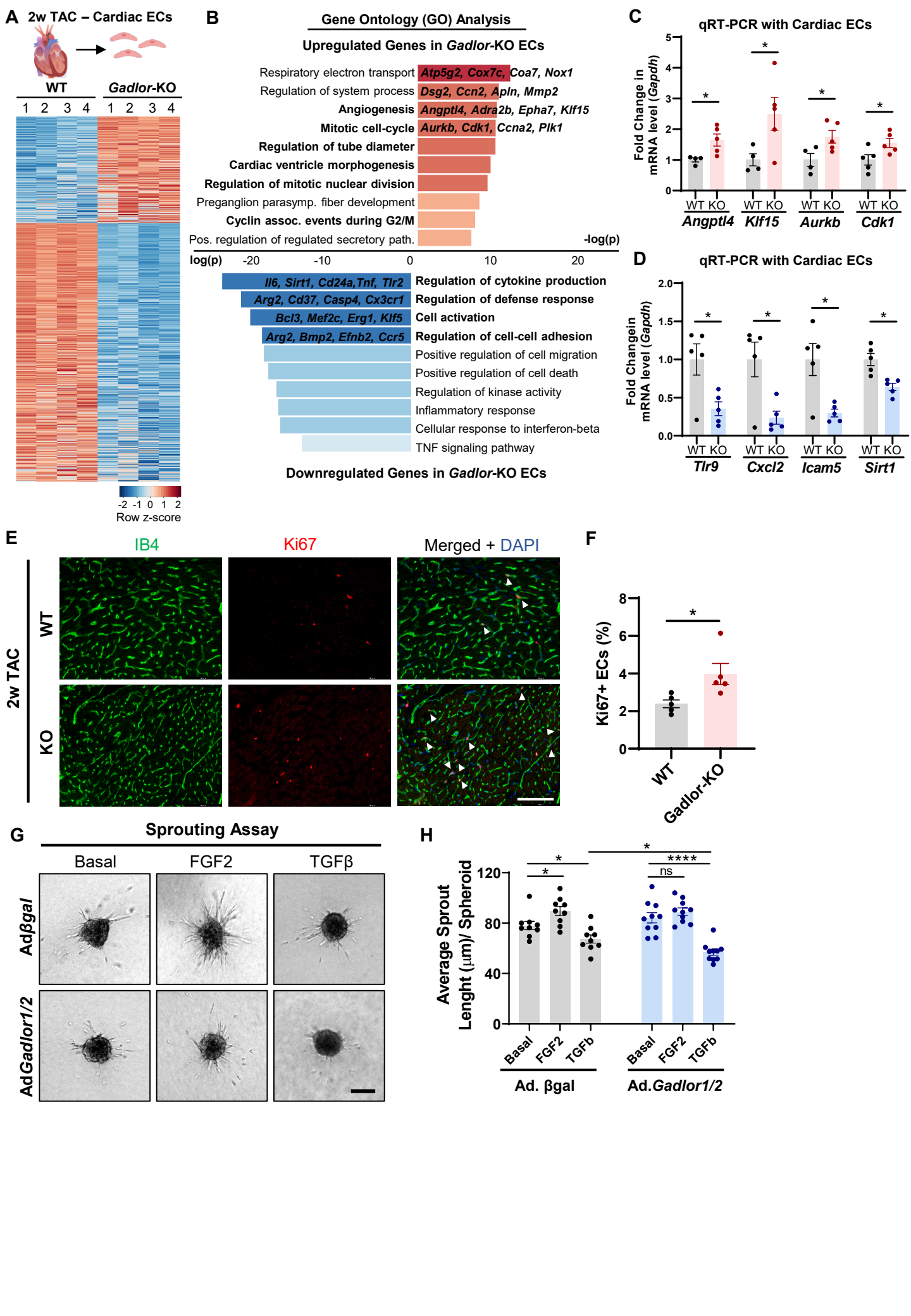
A
2w TAC – Cardiac ECs
WT
Gadlor-KO
1 2 3 4
1 2 3 4
-2 -1 0 1 2
Row z-score
B
Gene Ontology (GO) Analysis
Upregulated Genes in Gadlor-KO ECs
Respiratory electron transport
Atp5g2, Cox7c, Coa7, Nox1
Regulation of system process
Dsg2, Ccn2, Apln, Mmp2
Angiogenesis
Angptl4, Adra2b, Epha7, Klf15
Mitotic cell-cycle
Aurkb, Cdk1, Ccna2, Plk1
Regulation of tube diameter
Cardiac ventricle morphogenesis
Regulation of mitotic nuclear division
Preganglion parasymp. fiber development
Cyclin assoc. events during G2/M
Pos. regulation of regulated secretory path.
-log(p)
log(p) -20 -10 0 10 20
Il6, Sirt1, Cd24a,Tnf, Tlr2
Regulation of cytokine production
Arg2, Cd37, Casp4, Cx3cr1
Regulation of defense response
Bcl3, Mef2c, Erg1, Klf5
Cell activation
Arg2, Bmp2, Efnb2, Ccr5
Regulation of cell-cell adhesion
Positive regulation of cell migration
Positive regulation of cell death
Regulation of kinase activity
Inflammatory response
Cellular response to interferon-beta
TNF signaling pathway
Downregulated Genes in Gadlor-KO ECs
C
qRT-PCR with Cardiac ECs
Fold Change in mRNA level (Gapdh)
WT KO
Angptl4
Klf15
Aurkb
Cdk1
D
qRT-PCR with Cardiac ECs
Fold Changein mRNA level (Gapdh)
Tlr9
Cxcl2
Icam5
Sirt1
E
IB4
Ki67
Merged + DAPI
2w TAC
WT
KO
F
Ki67+ ECs (%)
WT
Gadlor-KO
G
Sprouting Assay
Basal
FGF2
TGFβ
Adβgal
AdGadlor1/2
H
Average Sprout Lenght (μm)/ Spheroid
Basal
FGF2
TGFb
Ad. βgal
Ad.Gadlor1/2
ns
****

**Figure 4: Deletion of *Gadlor* lncRNAs induces angiogenesis and expression of cell cycle genes in cardiac ECs after pressure-overload.**

**A.** Heatmap showing differentially regulated genes revealed by bulk RNAseq of cardiac endothelial-cells after 2-weeks TAC. **B.** Bar plots showing the gene-ontology (GO) analysis of upregulated and downregulated genes in *Gadlor*-KO ECs compared to WT ECs after 2-weeks TAC (Red: Upregulated in *Gadlor*-KO, Blue: Downregulated in *Gadlor*-KO). Some exemplary genes were listed for selected GO-terms. **C-D.** Validation of selected genes from RNAseq data with qRT-PCR in isolated cardiac ECs after 2 weeks of TAC (Red: Upregulated in *Gadlor*-KO, Blue: Downregulated in *Gadlor*-KO). **E.** Representative immunofluorescence images of cardiac tissue samples stained with IB4 (Isolectin B4 coupled with Alexa Fluor 488) and Ki67 (coupled with Alexa Fluor 555) in 2-week TAC samples from *Gadlor*-KO and WT littermates, Scale bar: 100 µm. (Arrows showing Ki67+ ECs) **F.** Quantification of Ki67 positive endothelial-cells percentage (Ki67+ ECs%). **G.** Representative images of sprouting assay with C166 mouse ECs after adenovirus treatment (Ad*βgal* and Ad*Gadlor1/2*) followed by 24 hour FGF2 and TGFβ treatment. 3-dimentional (3D) collagen matrix embedded spheroids were allowed to form sprouts for 24 hours. Scale bar: 100 µm. **H.** Quantification of average length of sprouts per each spheroid.

Data are shown as mean±SEM. Data normality was evaluated with Shapiro-Wilk test and p-values were calculated with Student's t-test for comparing two groups. For grouped analysis, p-values were evaluated with two-way ANOVA followed with Fisher's LSD post-doc test. *p-value<0.05, **p-value<0.01, ***p-value<0.001, ****p-value<0.0001.

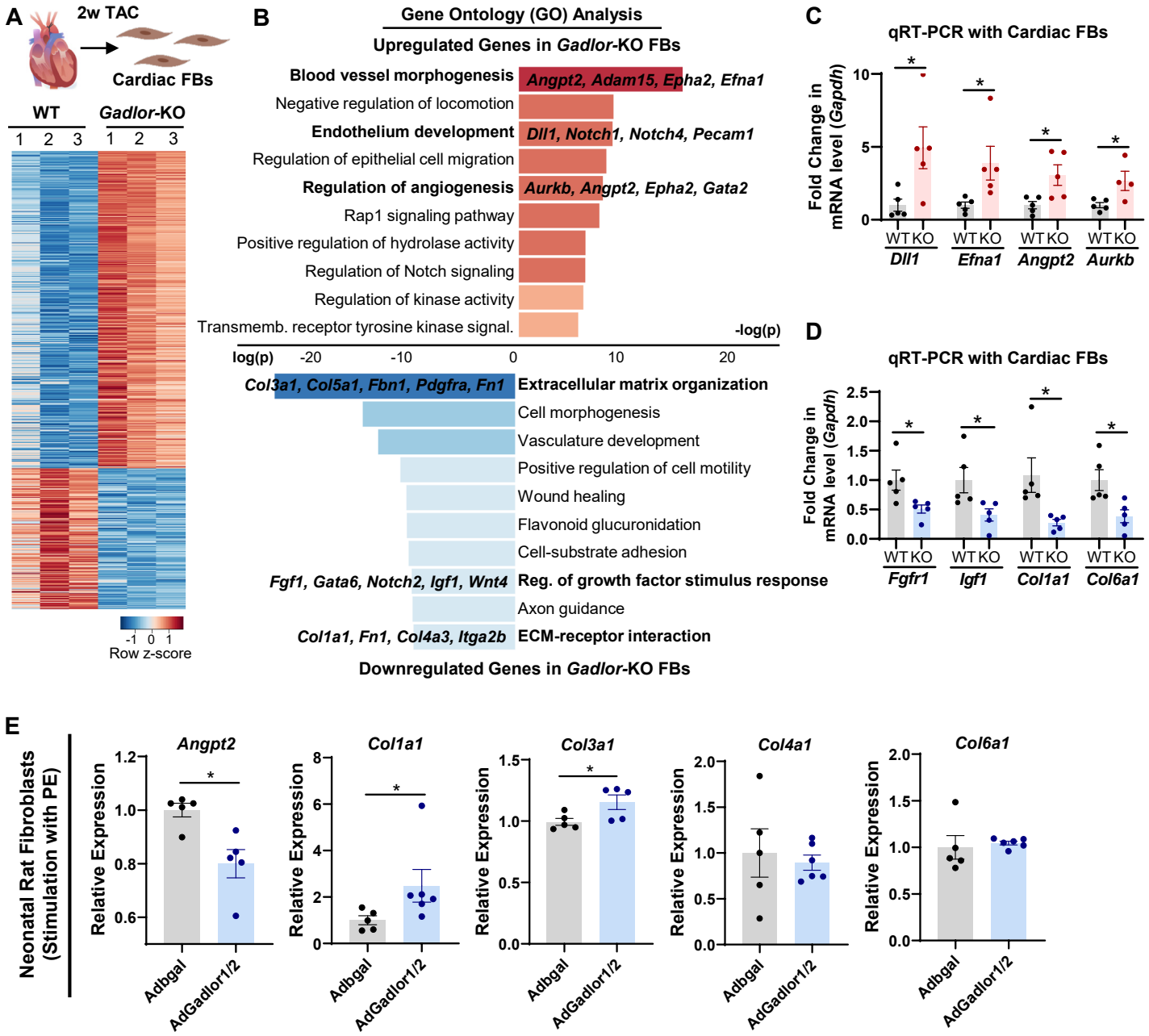


**Figure 5: RNA sequencing of *Gadlor*-KO cardiac FBs showed less induction of fibrosis-associated genes after TAC.**

**A.** Heatmap showing differentially regulated genes analysed after bulk RNAseq of isolated cardiac fibroblasts after 2-weeks TAC. **B.** Bar plots showing the gene-ontology (GO) analysis of upregulated and downregulated genes in *Gadlor*-KO FBs after 2-weeks TAC (Red: Upregulated in *Gadlor*-KO, Blue: Downregulated in *Gadlor*-KO). Some exemplary genes were listed for selected GO-terms. **C-D.** Validation of selected genes from RNAseq data with qRT-PCR in isolated adult cardiac FBs after 2 weeks of TAC (Red: Upregulated in *Gadlor*-KO, Blue: Downregulated in *Gadlor*-KO). **E.** qRT-PCR of selected genes in neonatal rat fibroblasts (NRFB) overexpressing *Gadlor* lncRNAs after *Gadlor1/2* adenovirus treatment (*βgal* as control) followed by phenylephrine (PE) stimulation (100 µM, 24 hours). Data are shown as mean±SEM. Data normality was evaluated with Shapiro-Wilk test and p-values were calculated with Student's t-test for parametric and Mann-Whitney test for non-parametric assessment. *p-value<0.05.

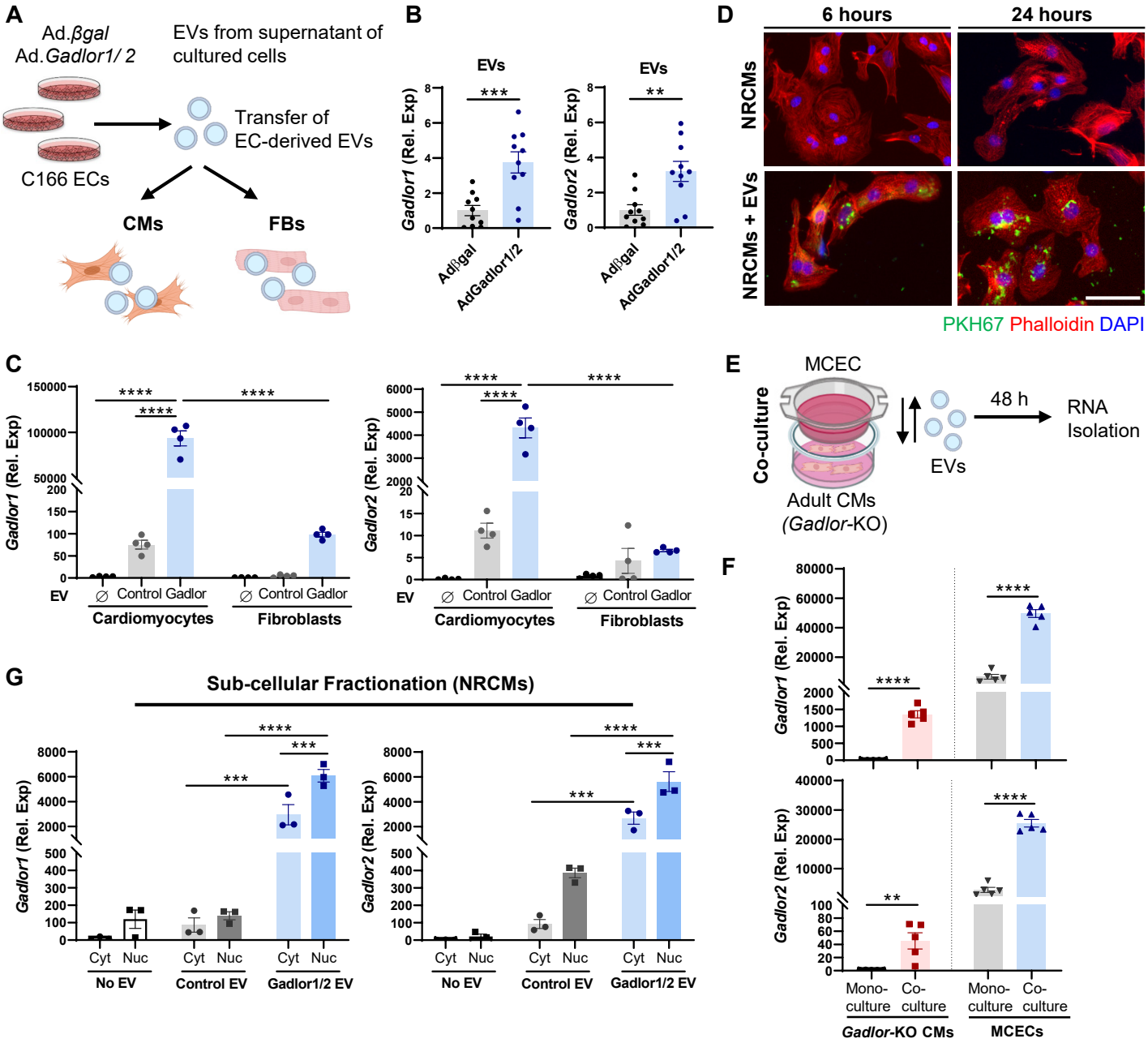


**Figure 6: Secreted *Gadlor* lncRNAs are transferred to cardiomyocytes via endothelial-derived EVs.**

**A.** Schematic representation of experimental design which EVs isolated from C166 supernatant was transferred to NRCMs and NRFBs, separately. **B.** Validation of *Gadlor1* and *Gadlor2* overexpression in isolated EVs. **C.** RT-qPCR detection of *Gadlor1* and *Gadlor2* after transferring control EVs (Ad*βgal* treated) and *Gadlor*-EVs (Ad*Gadlor1/* 2 treated) isolated from C166 mouse ECs into neonatal rat cardiomyocytes (NRCMs) or into neonatal rat fibroblasts (NRFBs). The samples were collected after 6 hours of EV-containing media incubation. **D.** Visualization of NRCMs that were incubated with PKH67-labelled (green) EVs isolated from C166 ECs for 6 hours and 24 hours. Staining was performed with Phalloidin (red) and DAPI (blue). Scale bar: 50 µm. **E.** Scheme of co-culture experiment with transwell (1 µm – allows EV transfer). MCEC on top cultured with *Gadlor*-KO CMs in the bottom well without direct cell contact. **F.** RT-qPCR detection of *Gadlor1* and *Gadlor2* in isolated *Gadlor*-KO CMs and MCEC mouse ECs after 48 hours of mono-culture and co-culture state. Data are shown as mean±SEM. Data normality was evaluated with Shapiro-Wilk test and p-values were calculated with Student's t-test or one-way ANOVA with Fisher's LSD post-hoc test were applied for comparing two or multiple groups, respectively. Two-way ANOVA with Fisher's LSD post-hoc test was applied for grouped analysis when applicable. *p-value<0.05, **p-value<0.01, ***p-value<0.001, ****p-value<0.0001.

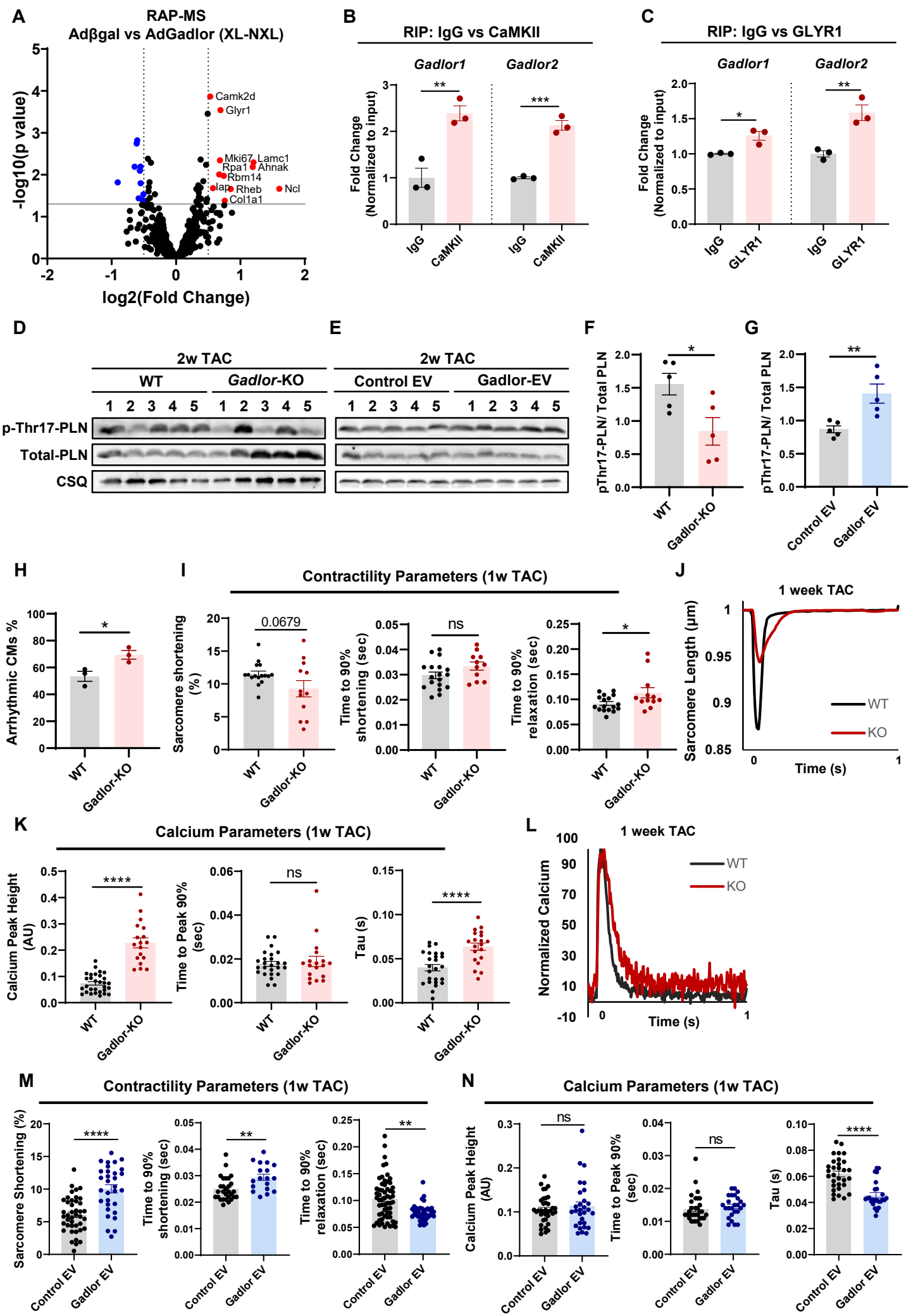
A
RAP-MS
Adβgal vs AdGadlor (XL-NXL)
-log10(p value)
log2(Fold Change)
Camk2d
Glyr1
Mki67
Lamc1
Rpa1
Ahnak
Rbm14
Iap
Rheb
Ncl
Col1a1
B
RIP: IgG vs CaMKII
Gadlor1
Gadlor2
Fold Change (Normalized to input)
IgG
CaMKII
C
RIP: IgG vs GLYR1
GLYR1
D
2w TAC
WT
Gadlor-KO
p-Thr17-PLN
Total-PLN
CSQ
E
Control EV
Gadlor-EV
F
pThr17-PLN/ Total PLN
G
H
Arrhythmic CMs %
I
Contractility Parameters (1w TAC)
Sarcomere shortening (%)
0.0679
ns
Time to 90% shortening (sec)
Time to 90% relaxation (sec)
J
1 week TAC
Sarcomere Length (μm)
Time (s)
K
Calcium Parameters (1w TAC)
Calcium Peak Height (AU)
Time to Peak 90% (sec)
Tau (s)
L
Normalized Calcium
M
N

**Figure 7. *Gadlor* lncRNAs bind to calcium/calmodulin-dependent protein kinase type II - subunit delta in cardiomyocytes.**

**A.** Volcano plot indicating the identified interaction partners of *Gadlor1* and *Gadlor2* in cardiomyocytes with RNA-antisense purification coupled with mass spectroscopy (RAP-MS). HL1 cardiomyocytes treated with *βgal* and *Gadlor1/2* adenovirus to identify interaction partners of *Gadlor* lncRNAs (Fold change (FC) threshold 1.2 and p-value < 0.05). UV crosslinking was used to stabilize protein:RNA interactions and non-crosslinked (N-XL) samples were used as background and removed from crosslinked (XL) samples for each indicated condition. **B.** RNA immunoprecipitation (RIP) performed with anti-IgG and anti-CaMKII antibodies incubated with HL-1 cardiac muscle cell lysate to validate the interaction of target RNAs. RT-qPCR analysis showing the enrichment of *Gadlor1* and *Gadlor2* compared to IgG controls. Data was normalized to input RNA expression. (n=3 for each condition) **C.** RNA immunoprecipitation (RIP) performed with anti-IgG and anti-GLYR1 antibodies with HL-1 cardiac muscle cell lysate to validate the interaction of target RNAs. RT-qPCR analysis showing the enrichment of *Gadlor1* and *Gadlor2* compared to IgG controls. Data normalized to input RNA expression. (n=3 for each condition) **D.** Exemplary Western blots of phospho-Thr17-PLN and total PLN with CSQ as loading control in WT and *Gadlor*-KO heart tissue samples after 2 weeks TAC. **E.** Exemplary Western blots of phospho-Thr17-PLN and total PLN with CSQ as loading control in control-EV and Gadlor-EV treated mice heart tissue samples after 2 weeks TAC. **F-G.** Quantification of Western-blots. **H.** Percentage of isolated adult WT and *Gadlor-KO* cardiomyocytes with arrhythmic phenotype after 1-week TAC recorded by Multicell HT system (Ion-Optix) Cell number≥30 in each condition. Sarcomere contractility **(I-J)** and calcium transient **(K-L)** measurements were recorded in parallel with Multicell HT system with continuous perfusion of basal media on isolated adult CMs after 1-week TAC. **I.** Contractility parameters including sarcomere shortening (%), time to 90% shortening (sec, systolic) and relaxation (sec, diastolic). **J.** Representative sarcomere contraction recordings of WT and *Gadlor*-KO CMs. **K.** Calcium parameters including calcium peak height (arbitrary units, AU), time to 90% peak of fura-2, AM ratio increase and decay time constant as an indication of speed of recovery (tau, seconds). **L.** Representative calcium transient recordings of WT and *Gadlor*-KO mice shown as normalized levels of calcium (%). **M.** Sarcomere function (sarcomere shortening (%), time to 90% shortening and relaxation (s)) and **N.** calcium transient (Calcium peak height, arbitrary units (AU), time to 90% peak of fura-2, AM ratio increase and decay time constant (tau, seconds). Recordings were obtained in adult cardiomyocytes isolated from WT mice followed treated by incubation of control-EV (Ad.βgal) and *Gadlor1/2*-EVs (Ad.Gadlor1 and Ad.Gadlor2) for 4 hours.

Data are shown as mean±SEM. Data normality was evaluated with Shapiro-Wilk test and p-values were calculated with Student's t-test (Mann-Whitney for non-parametric) for comparing two groups. *p-value<0.05, **p-value<0.01, ***p-value<0.001, ****p-value<0.0001.

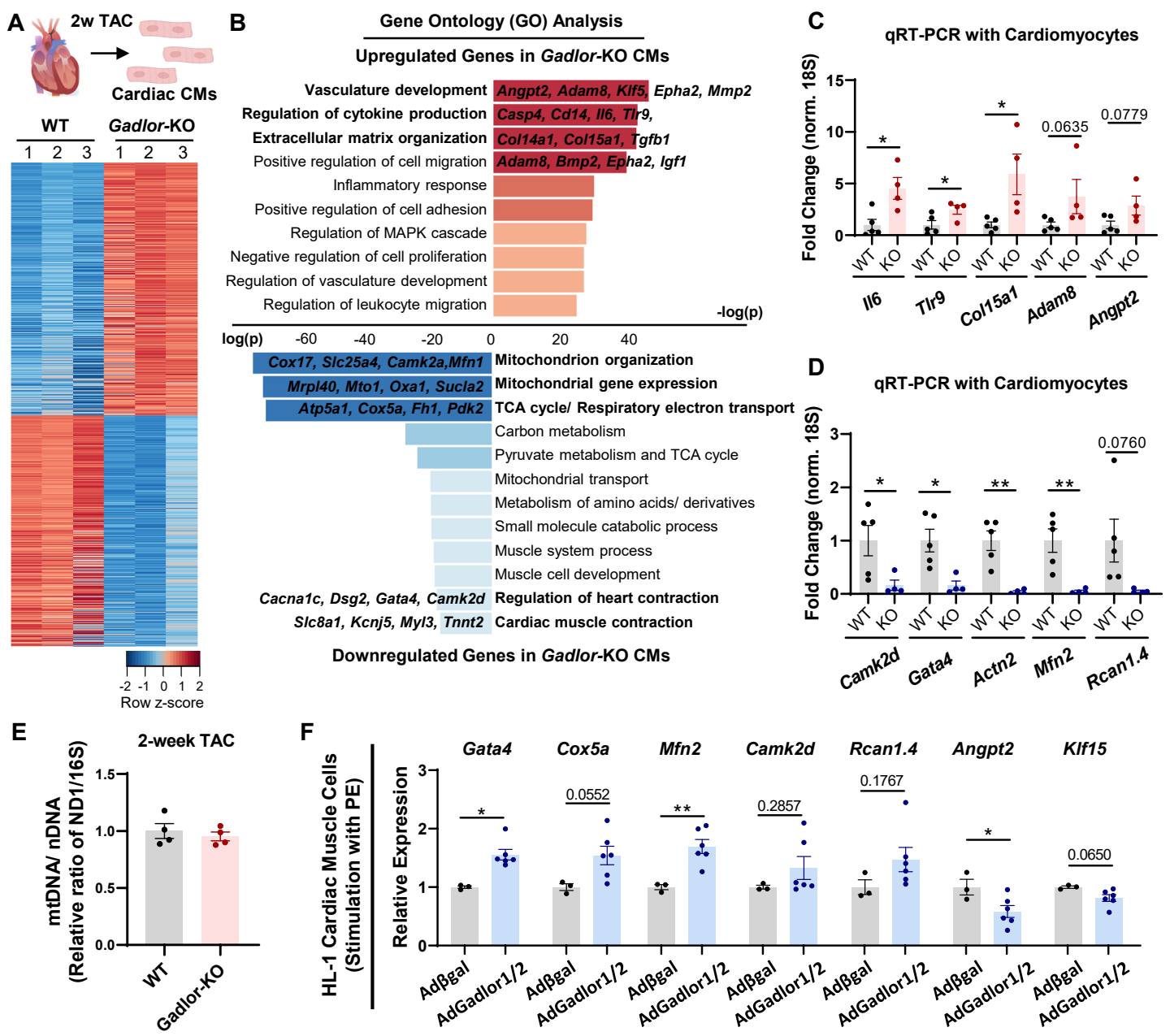


**Figure 8. Deletion of *Gadlor1* and *Gadlor2* affects gene expression in cardiomyocytes.**
**A.** Heatmap showing differentially regulated genes analysed after bulk RNAseq of isolated cardiomyocytes after 2-weeks TAC. **B.** Bar plots showing the gene-ontology (GO) analysis of upregulated and downregulated genes in *Gadlor*-KO CMs after 2-weeks TAC. (Red: Upregulated in *Gadlor*-KO, Blue: Downregulated in *Gadlor*-KO). Some exemplary genes were listed for selected GO-terms. **C-D.** Validation of selected upregulated and downregulated genes from RNAseq data with qRT-PCR. **E.** Analysis of mitochondrial DNA (mtDNA) to nuclear DNA (nDNA) ratio determined via quantitative PCR by using WT and *Gadlor-KO* heart tissue DNA samples isolated 2-weeks after TAC. Measurement of ND1 and 16S rRNA DNA expression was used to determine the mtDNA/ nDNA ratio. **F.** qRT-PCR of selected genes in HL-1 cardiac muscle cells overexpressing *Gadlor* lncRNAs after *Gadlor1/2* adenovirus treatment (*βgal* as control) followed by phenylephrine (PE) stimulation (100 µM, 24 hours). Data are shown as mean±SEM. Data normality was evaluated with Shapiro-Wilk test. *p*-values were calculated with Student's t-test for parametric (or Mann-Whitney for non-parametric) for comparing two groups. *p-value<0.05, **p-value<0.01, ***p-value<0.001, ****p-value<0.0001.

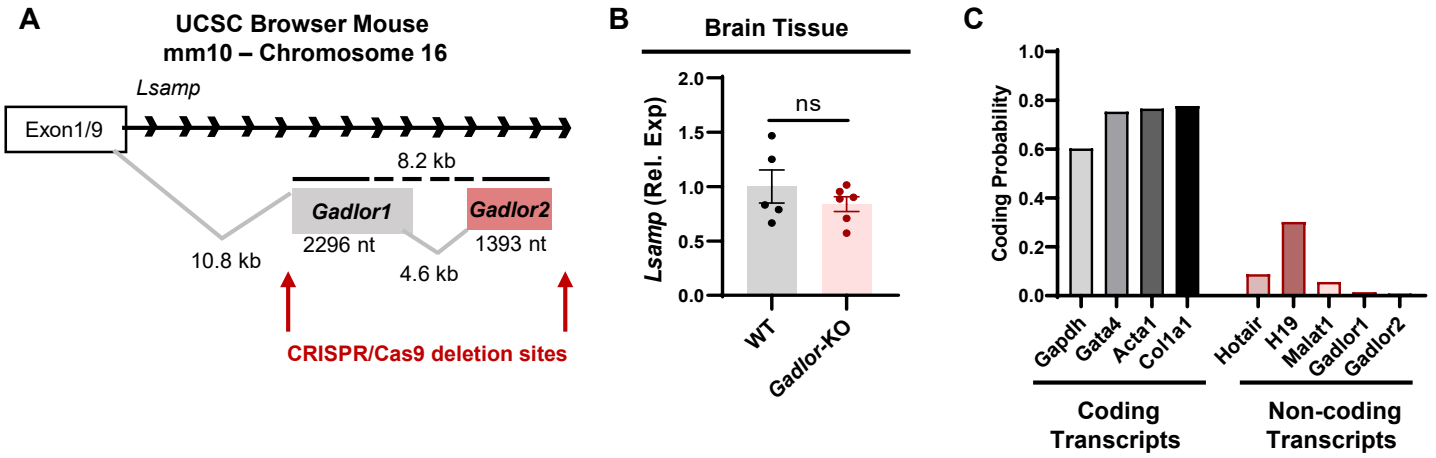


**Supplement Figure 1: *Gadlor1* and *Gadlor2* are non-coding transcripts that are located in the intronic region of the *Lsamp* gene.**

**A.** Representative scheme of *Gadlor1* and *2* locus and neighbor genes in UCSC Genome Browser (mm10) and the position of the CRISPR/Cas9 deletion sites used to generate *Gadlor*-KO mouse line. *Gadlor* lncRNAs are embedded in the intronic region of the *Lsamp* gene.
**B.** Systemic deletion of the whole region containing *Gadlor* lncRNAs did not affect the expression of neighbor gene *Lsamp,* which is mainly expressed in brain tissue. (Relative expression to *Gapdh*)
**C.** Coding probability of *Gadlor1* and *Gadlor2* was evaluated with online Coding Potential Assessment Tool (CPAT - http://lilab.research.bcm.edu/), and compared with coding transcripts and well-known lncRNAs for validation that revealed *Gadlor1* and *Gadlor2* are non-coding transcripts.

**A** **AK037972 (*Gadlor1*)**

```
#=======================================
# Aligned_sequences: 2
# Gap_penalty: 10.0
# Extend_penalty: 0.5
#
# Length: 578
# Identity:     268/578 (46.4%)
# Similarity:   268/578 (46.4%)
# Gaps:         259/578 (44.8%)
# Score: 740.5
#=======================================
H   1 AAATTGTCTAGAA-TGTGGCAGTTTAAAAACACATCTACATTGATCTACA     49
      |||||||.||||| |||||||.|||||||.|||.||..||||||||||.
M   1 AAATTGTTTAGAACTGTGGCACTTTAAAAGCACCTCGGCATTGATCTACT     50

   50 GTCTCAAGGTCCCAC--CTTTGTGTTACTTTTAGAATTTGTAGATGGATG     97
      ..|||.||.||.|||  ||.||||.||||||||||.||||||||||||.
   51 AACTCTAGATCTCACCTCTCTGTGCTACTTTTAGAGTTTGTAGATGGATA    100

   98 TTATTCAGCA-AGGATGACTCATCTACATT-TGGTTTGTCAATTTGTTTT    145
      .|.|.||||| |||| ||.||||||||.|| ||  .||||.|||||||||
  101 CTGTCCAGCAGAGGA-GAGTCATCTACGTTCTG--ATGTCGATTTGTTTT    147

  146 CAAAGATCATA----TGTACATAGCGTCCT----TCGATCTTACTTTCCC    187
      ||.||||||.|    || ||||    ||||    |.|     |||.||||
  148 CAGAGATCAGACACTTG-ACAT----TCCTAGAGTGG-----ACTGTCCC    187

  188 TTTAAAATATGAAACTGATAATGACCTTGAAAAAGAT-------AGAATT    230
      |||||||||||||||...||||||.|||..|.||||||        |.|.||
  188 TTTAAAATATGAAACAAGTAATGGCCTACAGAAAGATTATGATAAAACTT    237

  231 TC----------------------------------------AG------    234
      ||                                        ||
  238 TCCAGTTTTTTGGCTTTTCCCTTCGGCCCTGACTGGATGTGTAGTCTACT    287

  235 --CCACAA--------------------------------------------    240
        ||||||
  288 TCCCACAATCCTGTATGTTACATGGTTCCCTACCCAGACCACTCCCTTTG    337

  241 ----------------------------------------GCATCCCA-    248
                                              ||||.|||
  338 CCCCACCCCAAAAATGGCTACTGGGCTTTCTCAATCATCTTGCATGCCAC    387

  249 ---------------------------------TGAA-------AT----    254
                                       ||||       ||
  388 CCCTCGCCTTCTTTTATGTTTCAGAGTTGTGTGTGAAGAATCACATTAGT    437

  255 --TAATGTATCCATACTTTTAACA--CTA-----GTATAC-----TTTAT    290
        ||.|||||.|.|.||||| |||  |||     ||.|||     |||||
  438 GATACTGTATGCTTTCTTTT-ACAATCTATTTACGTTTACACATATTTAT    486

  291 CTTCTTATTT-CA-AATGCTC--TGTCTCC--------------------    316
      .||..||||| || |.|.|||  |||.|.|
  487 TTTTATATTTACATATTTCTCATTGTTTACCAGTTGGCAATAGTGATATT    536

  317 TT---------CTGTCCA--TTACTTCC    333
      ||         ||.|.||  ||||||||
  537 TTGTGAGCTGACTTTACATTTTACTTCC    564
```

**B** **AK038629 (*Gadlor2*)**

```
#=======================================
# Aligned_sequences: 2
# Gap_penalty: 10.0
# Extend_penalty: 0.5
#
# Length: 913
# Identity:     656/913 (71.9%)
# Similarity:   656/913 (71.9%)
# Gaps:         130/913 (14.2%)
# Score: 2336.5
#=======================================
H   1 AAAAAGAAAATTTGGA-AGATGCTCAAATAGGA-TTGATAGAGGTTCATT     48
      ||.||.||||||||| || |||.||.|||||| ||| .||.|..|||..
M  34 AAGAATAAAATTTGGACAG-TGCACACATAGGACTTG-CAGGGACTCACA     81

   49 TTGTGTCATATTTT-CGCTTTATATGGATGTTGATATGTTCTCAGAATAA     97
      .||||||||||||| |.||||.||||.||||||||||||.||||||| |
   82 GTGTGTCATATTTTGCACTTTTTATGAATGTTGATATGTTTTCAGAAT-A    130

   98 ATTTATAACTGCAATAGAAAATGGAATGACTATTGATTATTTTTTAGTTA    147
      ||||||||||||||.|||||..|||||.||||||||||..||||||||.
  131 ATTTATAACTGCAATTGAAAACTGAATGGCTATTGATTAAATTTTAGTTT    180

  148 CCCAAACTAATTGTCATATAAAGCTTTGTAAAT-CTTTTA-AAATGAGTA    195
      |..|||||||||.||||||||||||..||||| |||||| |||  ||.|
  181 CAAAAACTAATTGACATATAAAGCTTCATAAATCCTTTTAGAAA--AGGA    228

  196 TGGGTGTAAATTAAAAACGAATTAAAGCAGAGGCTTATAAAGACACT---    242
      ||.||.||||||||||||.|||||.||||.||||||||||| |.|||
  229 TGAGTATAAATTAAAAACTAATTACAGCAAAGGCTTATAAA-ATACTCCA    277

  243 ATCTCCCCTTCAATGGGTTATGTATTTTTGTTGTGTGTTAGGAAGATATC    292
      || |||..|||.|| ||||||.||   .||||||.||.||.||||.|.|.
  278 AT-TCCAGTTCTAT-GGTTATATA---CTGTTGTATGCTATGAAGGTGTT    322

  293 TCTTGATCTCCACACCCAAAACTCCTTCC----------AAATGAACAAA    332
      .|||..|||.|..|..||||||||||.||          |.||||||
  323 CCTTTGTCTTCTTAATCAAAACTCCTGCCATAGAATTAAATATGAAC---    369

  333 GGCCTACACACAAAAATTATTTCAATTGCTAATAGCCAGTTTTTAT----    378
            ||.||||..||||.||||||||||....|.|||.|||
  370 --------CATAAAAGATATTTTAATTGCTAATGATTACTTTATATATAG    411

  379 ------TTTTCAAAAGTAAATGCTTTCTTTTTTTGAAAAGTAAATATAAC    422
            |||||||.||                     |||  .|||||.
  412 TATCCCTTTTCAAGAG----------------------AGT--TTATAAG    437

  423 TATTTTAACAAAGTAAGATTTAAAAA---AAAAAACAACTCAGAAAAAAG    469
      .|||||.|...|||||.|||||||||   ||||||.|||      |.|||
  438 AATTTTTAATCAGTAATATTTAAAAATTTAAAAAAGAAC------AGAAG    481

  470 T--GCCAT------GCAG-AGATAACAGGGCTGATCTGTCTGTTATCTGC    510
      |  |||||      |||| ||| |.||      || ||.|.||||||||.
  482 TGGGCCATGTTAAGGCAGCAGA-ACCA------AT-TGCCAGTTATCTGT    523

  511 AGCCTCTATCCTTACTGTTAACAAGCCTTTTATCTTTGAAGACACTAAAC    560
      |.||||||||||..||.|||.||||||||||.|||.||||||||||||.|
  524 AACCTCTATCCTTGATGCTAATAAGCCTTTTACCTTCGAAGACACTAAGC    573

  561 ATCTGGGATCTAAGCACTGACACCTATTAGTTACAGTGGTTTCCTTTTAC    610
      ||||||||||||||.|.||||||||||||||||||.||||||||||||||
  574 ATCTGGGATCTAAGTAGTGACACCTATTAGTTACAATGGTTTCCTTTTAC    623

  611 CTTTCTAAACTATCTGATAGATAAACCTCCAGGAATCCTACAAAATTAGG    660
      | ||||||.|.||||||||||||||||||||||||||||.||||||||.|.
  624 C-TTCTAAGCAATCTGATAGATAAACCTCCAGGAATCCCACAAAATTGGA    672

  661 CCCTTAATTGACCAAACGAATGTCTGTCTCTCTTTTTCAATCTAAATCAA    710
      ||||||||||||||||.||||||.||||||||||||||.||.|.||||||..|
  673 CCCTTAATTGACCAAATGAATGGCTGTCTCTCTTTTACAGTATAAATTGA    722

  711 AAAG-GAGTTTGCTCCTAGGAG--ATGAGATGATGTACAGTGGAAAAAAA    757
      |||| ||||||||||.|.|||  |.||.||.|..||    |||||.|||
  723 AAAGTGAGTTTGCTCCCATGAGGTAAGACATAACTTA----GGAAAGAAA    768

  758 TATTTCA-GCTGCAACTCCACTGGTAACCGTCAATGTGACCTTATAATCT    806
          ||| ||||..||||||||.|..| |.|.|.||||.||||.||||||
  769 ----TCACGCTGAGACTCCACTTGCCA-CATTAGTGTGCCCTTGTAATCT    813

  807 CCCC-----CCAATTTATTCCCA-AAACAGCTA--CCAAAGTGATCTTTC    848
      |.||     |||       |||| .||||| ||  .|||||||||..|||
  814 CACCAAAAGCCA-------CCCACCAACAG-TAGGACAAAGTGATTCTTC    855

  849 TAAAACCCACATC    861
      ||||||.||||||
  856 TAAAACGCACATC    868
```

**C**

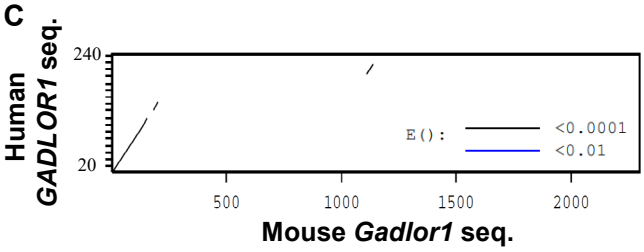


**D**

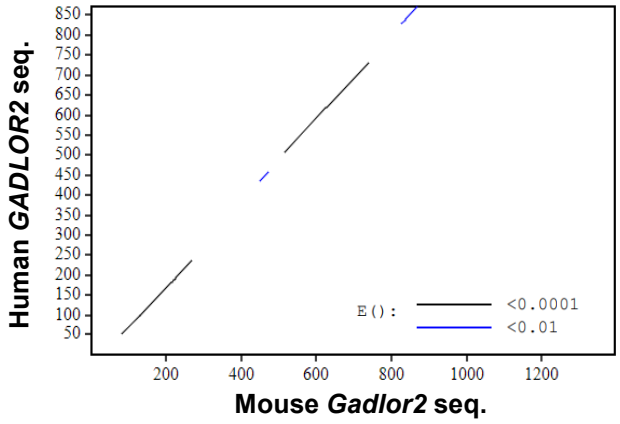


**Supplement Fig 2: Conservation levels of *Gadlor1/2* between mouse and human genome.**

**A-B.** Assessment between human (H) and mouse (M) *Gadlor1/2* in sequence conservation level evaluated with EMBOSS-Water local alignment tool (https://www.ebi.ac.uk/Tools/psa/emboss_water/), and **C-D.** visualization of pairwise local alignment with LALIGN DNA:DNA tool of University of Virginia (https://fastademo.bioch.virginia.edu/fasta_www2/fasta_www.cgi?rm=lplalign).

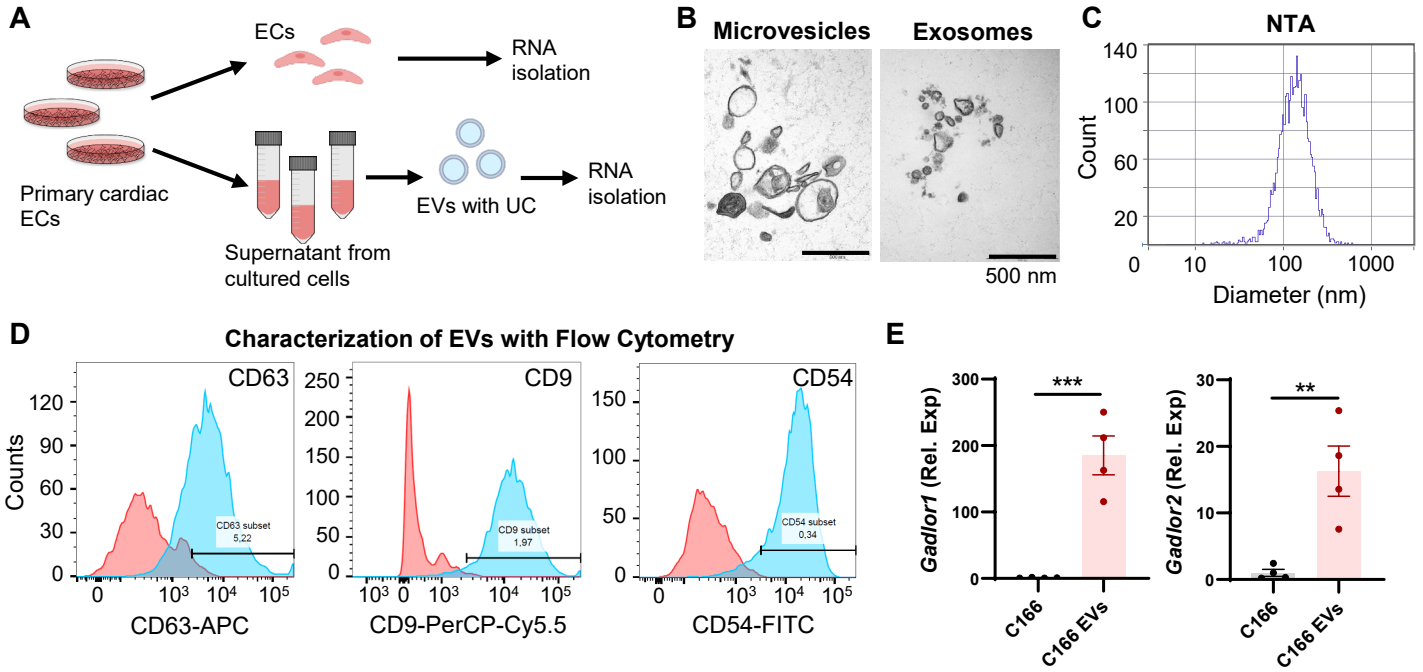


**Supplement Figure 3: *Gadlor* lncRNAs are mainly secreted in endothelial cells (EC) derived extracellular vesicles (EVs).**

**A.** Scheme depicting the experimental design of EV isolation with ultracentrifugation (UC) from cultured primary cardiac ECs. Characterization of cardiac EC-derived EVs by **B.** visualizing microvesicles and exosomes with electron microscopy (scale bar: 500 nm) and **C.** detecting the size in diameter (nm: nanometers) with Nanoparticle Tracking Analysis (NTA). **D.** Flow cytometry analysis of EV surface markers (CD63-APC, CD9-PerCP-Cy5.5 and CD54-FITC) on EC-derived EVs that were stained against markers (blue curve) and compared to isotype control (red curve). **E.** Expression of *Gadlor1* and *Gadlor2* in C166 mouse endothelial cell and in EVs derived from these cells.
Data are shown as mean±SEM. Data normality was evaluated with Shapiro-Wilk test and p-values were calculated with Student's t-test for parametric (or Mann-Whitney for non-parametric) assessment. *p-value<0.05, **p-value<0.01, ***p-value<0.001.

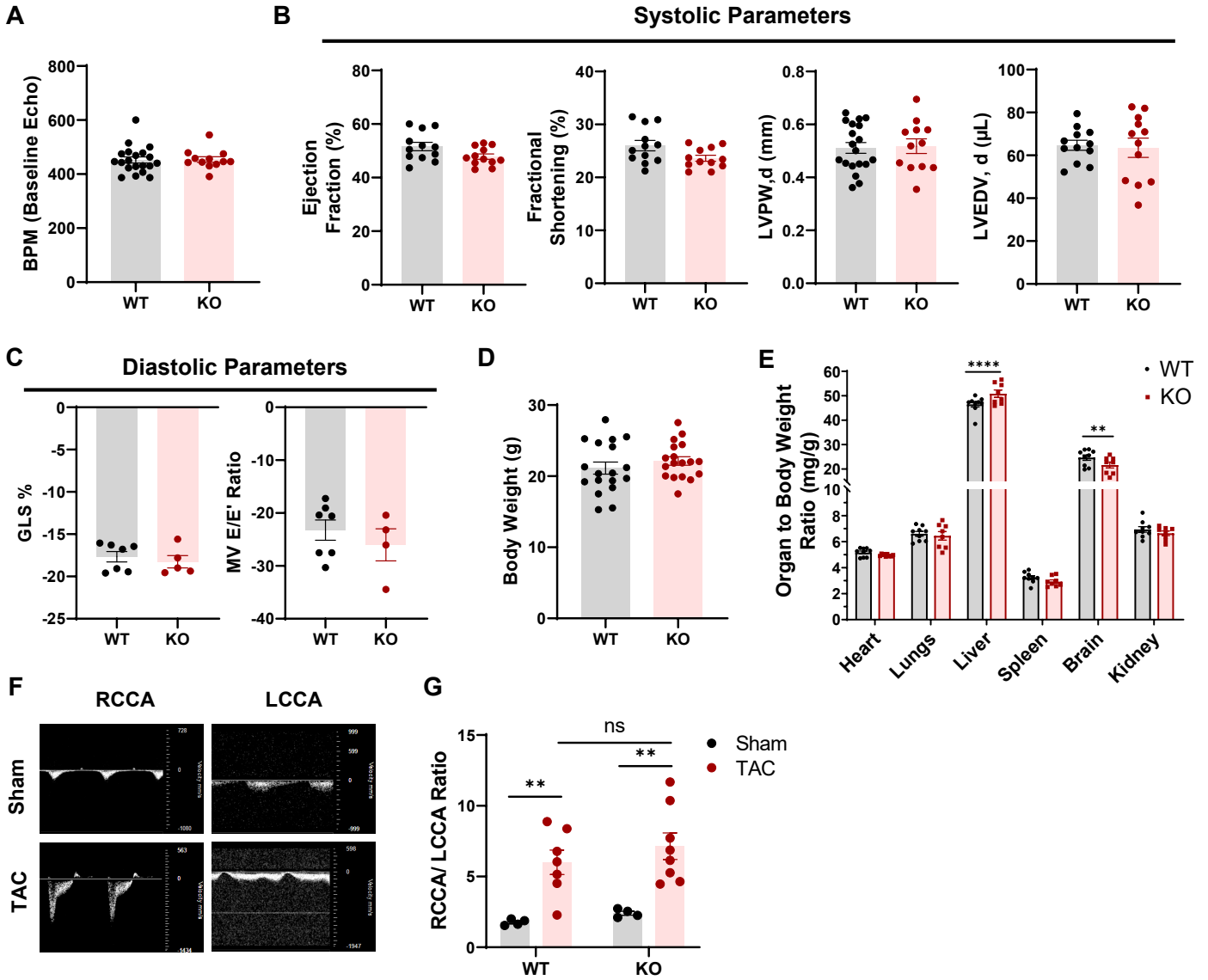


**Supplement Figure 4: Baseline phenotypic characterization of *Gadlor*-KO mice compared to wild-type (WT) littermates.**

**A.** Heart rate of WT and *Gadlor*-KO mice during echocardiography (BPM: beats per minute, n≥12). **B.** Analysis of systolic function parameters of left ventricle (LV) ejection fraction (%), fractional shortening (%), LV posterior wall thickness in diastole (mm) and LV end diastolic volume (µl) (n≥12). **C.** Analysis of diastolic function parameters, global longitudinal strain (GLS, %) and mitral valve (MV) E to E' ratio (n≥4). **D.** Body weight (g) of adult (9 weeks old) WT and *Gadlor*-KO animals (n≥18), and **E.** organ to body weight ratio (mg/g) of isolated organs including heart, lungs, liver, spleen, brain and kidney (n≥8). **F-G.** Representative images and quantification of flow measurement in right and left common carotid arteries (RCCA and LCCA) in sham (n≥4) and TAC (n≥7) mice to measure the strength of TAC operation in WT and *Gadlor*-KO animals.

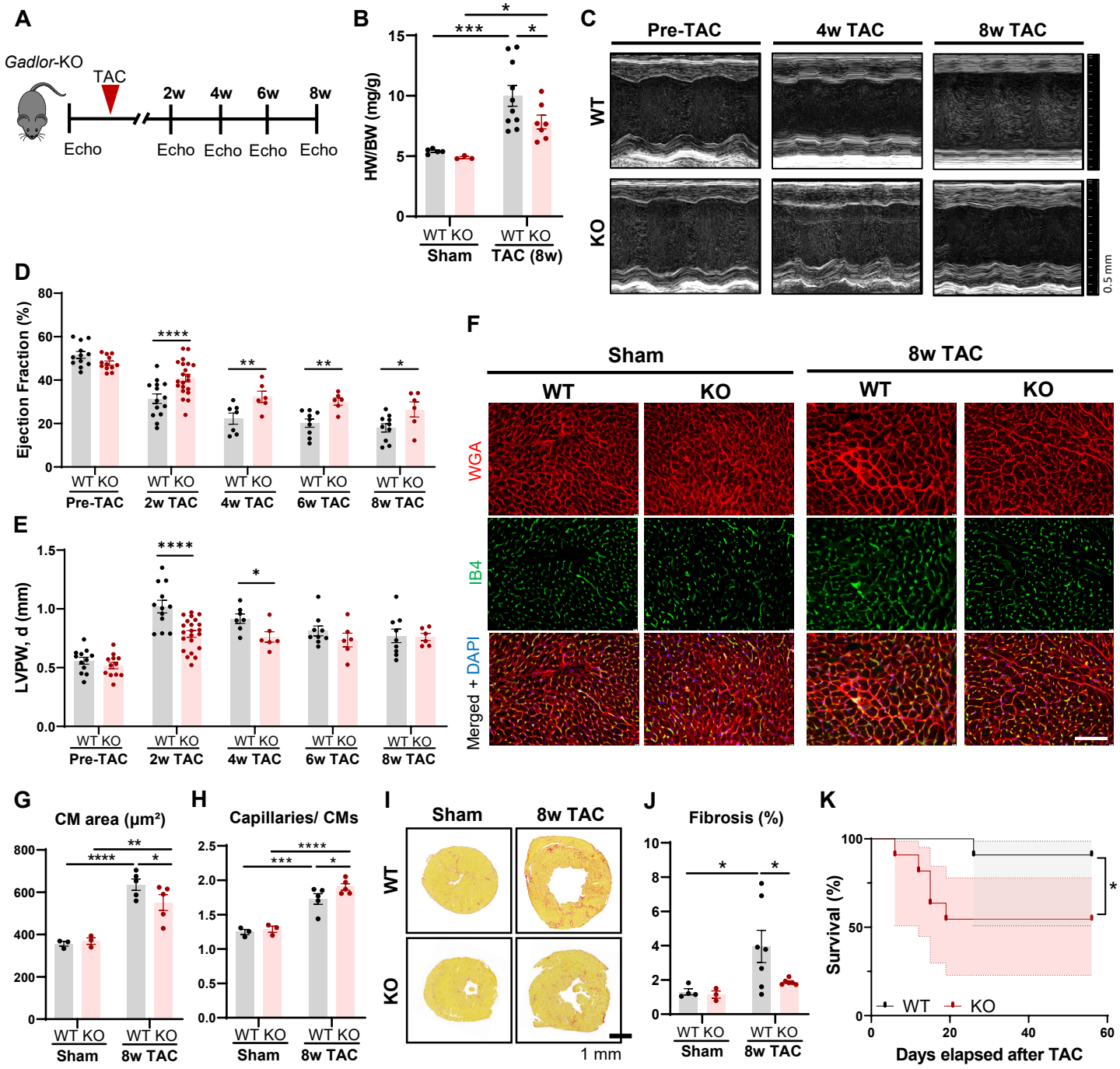


**Supplement Figure 5: *Gadlor*-KO mice showed higher mortality despite retaining better structural and physiological remodelling after persisting pressure-overload.**

**A.** Experimental design of long-term TAC operation for *Gadlor*-KO and WT littermates up to 8-weeks after TAC. **B.** Heart weight (miligrams) to body weight (grams) ratio (HW/BW) of *Gadlor*-KO and WT mice in age comparable sham (n≥3) and after 8-weeks TAC (n≥7). **C.** Representative echocardiography images of *Gadlor*-KO and WT mice before (pre-TAC) and after 4-weeks and 8-weels TAC shown in parasternal long axis mode, and analysis of **D.** left ventricle (LV) ejection fraction (EF%) and **E.** left ventricle (LV) posterior wall thickness in diastole (mm), (unpaired analysis). **F.** Representative immunofluorescence images of cardiac tissue samples stained with WGA (wheat-germ agglutinin coupled with Alexa Fluor 555) and IB4 (Isolectin B4 coupled with Alexa Fluor 488) in sham (n=3) and 8-week TAC (n=5) samples from *Gadlor*-KO and WT littermates, scale-bar: 100 µm. Quantification of **G.** cardiomyocyte cross-sectional area and **H.** myocardial capillary density per cardiomyocyte ratio. **I.** Representative Sirius-red fibrosis staining in cardiac tissue sections of sham (n≥3) and 8-week TAC (n≥6) mice (scale-bar: 1 mm) and **J.** quantification of fibrotic area (%). **K.** Survival of *Gadlor*-KO and WT mice after TAC (n=11). Probability of survival compared with log-rank (Mantel-Cox) test.
Data are shown as mean±SEM. Data normality was evaluated with Shapiro-Wilk test and p-values were calculated with Student's t-test for comparing two groups and two-way ANOVA for grouped analysis followed with Fisher's LSD post-hoc test. *p-value<0.05, **p-value<0.01, ***p-value<0.001, ****p-value<0.0001.

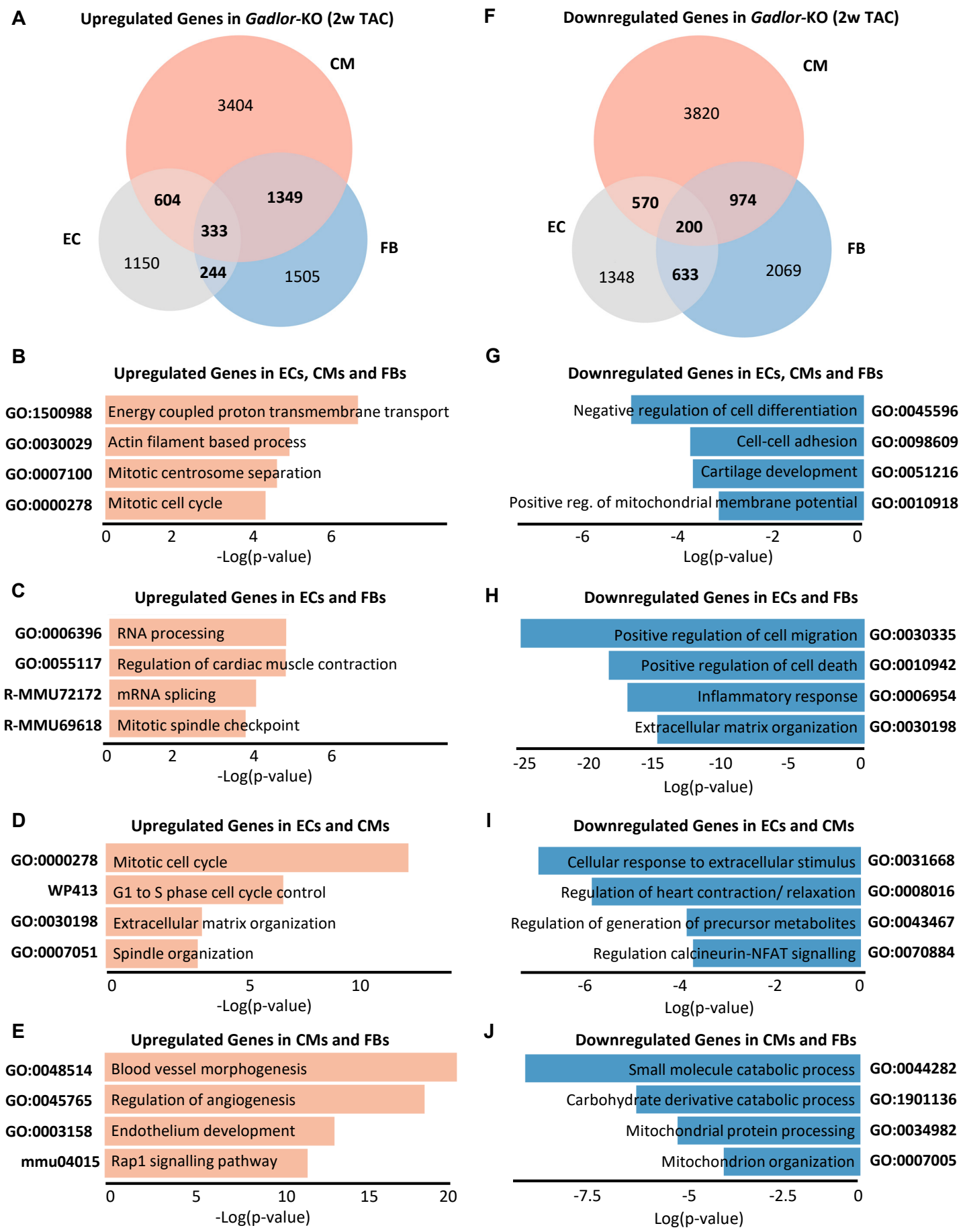


**Supplement Figure 6: Venn diagrams of differentially expressed genes in different cardiac cell types of *Gadlor*-KO mice compared to WT littermates after 2 weeks of TAC.**

**A.** Venn diagrams of upregulated genes in different cardiac cell types (CM: red, EC: grey, FB: blue) of *Gadlor*-KO mice compared to WT after 2-weeks TAC. The numbers indicating the number of genes in corresponding cell types. Genes were filtered as fold-change greater or equals to 1.2 for each condition. **B-E.** Gene ontology (GO) analysis of indicated intersections representing the overlapping upregulated genes in shown cell type of *Gadlor*-KO compared to WT littermates. **F-J.** Gene ontology (GO) analysis of indicated intersections representing the overlapping downregulated genes in shown cell type of *Gadlor*-KO compared to WT littermates. Bar plots showing selected GO-terms for each condition.

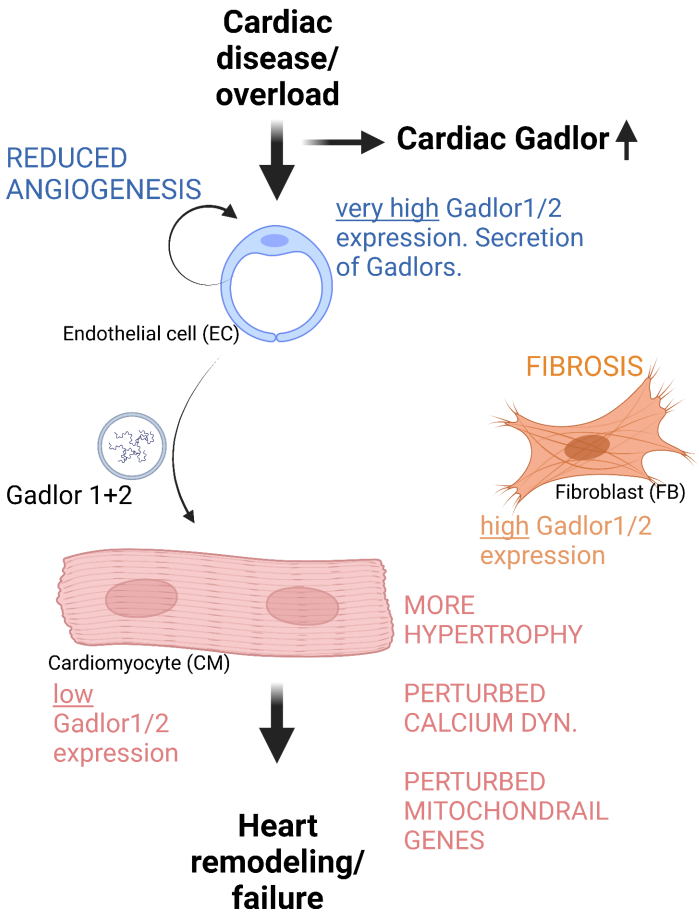


**Supplement Figure 7:** Graphical summary showing *Gadlor1* and *Gadlor2* lncRNAs expression and their effects (capitalized letters). The illustration was created with BioRender.com.